

Chapter 3

Exergy and Thermoeconomic Analysis of Power Plants, Refrigeration and Polygeneration Systems

Symbols

b	Specific exergy (kJ/kg)
B	Exergy rate (kW)
c	Specific cost (US\$/kWh, US\$/kJ or US\$/t)
C	Cost rate (\$/s)
C_{oi}	Cost of equipment i (US\$)
$C_{equip,i}$	Equipment i cost rate (US\$/s)
COP	Coefficient of performance
C_{turb}	Steam turbine cost rate (US\$/s)
E	Energy rate (kW)
f	The fraction of the rejected heat of the heat engine that is sent to the refrigeration system
f_i	Ratio of the exergy supplied to component i to the exergy consumed by the whole plant
f_l	Load factor
f_{om}	Annual operational and maintenance factor
f_t	Time factor
I	Investment cost rate (US\$/h)
LHV	Lower heating value (kJ/kg)
m	Mass flow rate (kg/s)
n	Annual interest rate
N_h	8760 h/year
P	pressure (bar)
P_o	Reference pressure (bar)
Q	Heat rate (kW)
r	Capital recovery period (year); parameter defined by Eq. 3.24
T_o	Reference temperature (K)
W	Power (kW)

Greek symbols

α	Relation between chemical exergy and lower heating value
β	Relation between heat rate and power
Δ	Variation
η_b	Exergy efficiency
η_e	Energy efficiency
$\theta, \bar{\theta}$	Carnot factor, average Carnot factor

Subscripts

abs	Absorption refrigerating system
air	Combustion air
b	Exergy
c	Compressor
cc	Combined cycle; combustion chamber
cd	Condenser
chilled water	Related to chilled water
cp	Compressor
cpi	Compressor inlet
cpo	Compressor outlet
crs	Compression refrigerating system
e	Electricity, Energy
ev	Evaporator
excess	Excess electricity
eg	Exhaust gas
equip	Equipment
fuel	Related to fuel
fuelcc	Fuel consumption in the gas turbine combustion chamber
fuelhrsg	Fuel consumption in the heat recovery steam generator
G	Related to the whole plant
gas	Natural gas
gases	Combustion gases
ge	Generator of the absorption chiller
gt	Gas turbine
hrsg	Heat recovery steam generator
i	Inlet, component i
o	Outlet
overall	Related to the whole plant
proc	Process
p	Pump; process
pump	Pump
pump i	Pump inlet
pump o	Pump outlet
plant	Related to plant
process	Related to process

products	Combustion products
$p1$	Steam demanded by process 1
$p2$	Steam demanded by process 2
q, Q	Heat/chilled water
sb	supplementary burning
sc	Steam cycle
st	Steam turbine
steam	Steam
t	Turbine
ti	Turbine inlet
to	Turbine outlet

Abbreviations

ABS	Absorption chiller
CC	Combustion chamber
CHP	combined heat and power unit
COND	Condenser
CONDP	Condensate pump
CIRCP	Circulating pump
CP	Air compressor
CT	Combustion turbine
CT	Cooling tower
D	Duct, Dimension
DB	Supplementary firing module
DEAR	Deaerator
ECON	Economizer
EVAP	Evaporator
FH	Fuel heater
GEE _q	Gas engine with equality method
GT	Gas turbine; turbine of the gas turbine
GTE _q	Gas turbine with equality method
GTE _x	Gas turbine with extraction method
HP	High pressure
HPCON	High pressure economizer
HPECO2	High pressure economizer 2
HPEVAP	High pressure evaporator
HPPUMP	High pressure feed pump
HPSHR	High pressure superheater
HPSHT1	High pressure superheater 1
HPST	High pressure section
HRSG	Heat recovery steam generator
IP	Intermediate pressure
IPCON	Intermediate pressure economizer
IPPUMP	Intermediate pressure feed pump

IPST	Intermediate pressure section
IPSHT	Intermediate pressure superheater
IPSTH2	Intermediate pressure superheater 2
IPVAP	Intermediate pressure evaporator
LP	Low pressure
LPEVAP	Low pressure evaporator
LPSHT	Low pressure superheater
LPST	Low pressure section
MMBtu	10 ⁶ Btu
OOO	Original operating condition
P	Pump
RH	Reheater
SHT	Superheater
ST	Steam Turbine
STE _q	Steam turbine with equality method
STE _x	Steam turbine with extraction method
TCR	Total cost rate (US\$/h)
TR	Ton of refrigeration (3.5 kW)
WTHT	Water heater

3.1 Introduction

The increasing interest in combined heat and power systems as well as combined cycle plants points out the need for identifying the best components configurations in order to maximize their exergy efficiency.

The exergy analysis of thermomechanical conversion plants aims to characterize how the fuel exergy is used and destroyed in the energy conversion processes that take place in these plants.

3.2 Exergy Analysis of Cogeneration and Combined Cycle Plants

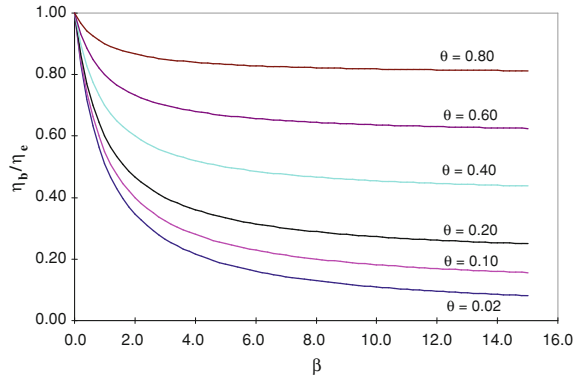
3.2.1 Exergy-Based Performance Parameters

Cogeneration systems are based on power generation plants that are modified to allow the utilization of the exergy associated to their thermal wastes.

The exergy performance of cogeneration systems can be derived from a general performance definition as discussed in [Chap. 2](#), and presented in [Eq. 3.1](#):

$$\eta = (\text{useful effect})/(\text{driving energy, exergy, etc.}) \quad (3.1)$$

Fig. 3.1 Behavior of η_b/η_e as a function of β for several values of θ [13]



Thus, the expressions of the energy (η_e) and exergy (η_b) performances are:

$$\eta_e = (W + Q) / E_{\text{fuel}} \quad (3.2)$$

$$\eta_b = (W + B_Q) / B_{\text{fuel}} \quad (3.3)$$

where B_Q is the exergy transferred to a process for heating or cooling (chilled water “production”) purposes.

Combining Eqs. 3.2 and 3.3, introducing the heat to work ratio, $\beta = Q/W$, the Carnot factor of the process, $\theta_p = 1 - T_0/T_p$, considering $B_Q = \theta_p Q$ and $\alpha = B_{\text{fuel}}/E_{\text{fuel}}$, one obtains:

$$\frac{\eta_b}{\eta_e} = \left(\frac{1 + \theta\beta}{1 + \beta} \right) \frac{1}{\alpha} \quad (3.4)$$

This expression allows to obtain easily the relation between the two performances parameters, given β , T_o , T_p , and knowing α .

Figure 3.1 shows the behavior of η_b/η_e as a function of β having θ as parameter, for a fuel with $\alpha = 1$. It is observed that when $\beta \rightarrow 0$ the relation between the performances tends to one because the useful effect of the system is the power generation (pure exergy). When $\beta \rightarrow \infty$ the relation between performances tends to θ , because the useful effect is essentially a heat transfer (heating/cooling). It can also be observed that for decreasing θ (in module), i.e., heat transfer processes with temperatures near to T_o (which is the case of an air conditioning systems), the relation between the performances drops for a same β , due to the lower exergy associated to the heat transfer.

Data presented in Fig. 3.1 are easily corrected for a fuel with $\alpha \neq 1$ by simply dividing the value of η_b/η_e of the graphic by the particular value of α (that can be obtained, for example, in the correlations presented by Szargut [1] and [2]).

Table 3.1 shows the values of W , Q , $\bar{\theta}$ (average Carnot factor), η_e , and η_b for four types of cogeneration systems.

Table 3.1 Characteristics of cogeneration system

Cogeneration system	\dot{W} (MW)	\dot{Q} (MW)	$ \bar{\theta} $	β	η_e	η_b
Gas turbine with HRSG and absorption chiller (COP = 1.1)	3.00	5.39	0.057	1.80	0.84	0.33
Internal combustion engine with HRSG	7.48	6.70	0.215	0.90	0.75	0.47
Combined cycle (GT + ST) with HRSG	26.03	32.21	0.273	1.24	0.77	0.46
Combined cycle (GT + ST) with compression chiller (COP = 4.5)	3.00	6.30	0.057	2.10	0.93	0.34

$T_o = 298$ K, *GT* gas turbine, *ST* steam turbine, *HRSG* heat recovery steam generator

Table 3.2 Expressions of η_{bi} and f_i

Component / parameter	η_{bi}	f_i
Compressor	$[\eta_b]_{cp} = \frac{B_{cpo} - B_{cpi}}{W_{cp}}$	$f_{cp} = \frac{W_{cp}}{B_{fuel}}$
Pump	$[\eta_b]_{pump} = \frac{B_{pumpo} - B_{pumpi}}{W_{pump}}$	$f_{pump} = \frac{W_{pump}}{B_{fuel}}$
Turbine	$[\eta_b]_t = \frac{W_t}{B_{ti} - B_{to}}$	$f_t = \frac{B_{ti} - B_{to}}{B_{fuel}}$
Combustion chamber	$[\eta_b]_{cc} = \frac{B_{products}}{B_{fuelcc} + B_{air}}$	$f_{cc} = \frac{B_{fuelcc} + B_{air}}{B_{fuel}}$
Heat recovery steam generator	$[\eta_b]_{hrsg} = \frac{\Delta B_{steam}}{B_{fuelhrsg} + \Delta B_{gases}}$	$f_{hrsg} = \frac{\Delta B_{gases} + B_{fuelhrsg}}{B_{fuel}}$
Compression refrigerating system	$[\eta_b]_{crs} = \frac{Q_{ev}\theta_{ev}}{W_{cp}}$	$f_{crs} = \frac{W_{cp}}{B_{fuel}}$
Absorption refrigerating system	$[\eta_b]_{abs} = \frac{Q_{ev}\theta_{ev}}{Q_{gc}\theta_{gc}}$	$f_{abs} = \frac{Q_{gc}\theta_{gc}}{B_{fuel}}$

In Table 3.1 it is interesting to notice the higher values of η_b for combined cycle and internal combustion engine systems with HRSG, due to the relative importance of the produced power.

Based on Eq. 3.1 it is possible to define the exergy efficiencies of the main components of a cogeneration and a power plant (compressor, turbine, pump, combustion chamber, steam generator, heat recovery steam generator, compression refrigerating system, and absorption refrigerating system). The expressions of these efficiencies are shown in Table 3.2.

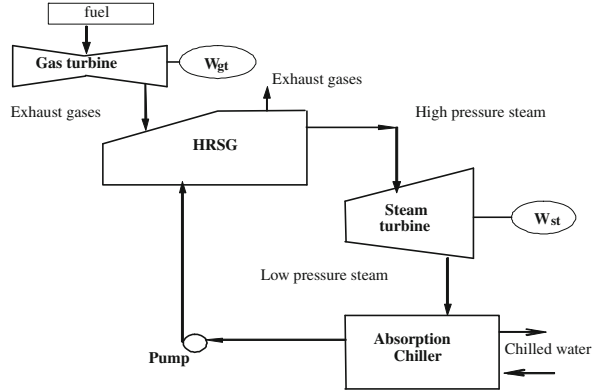
To characterize the importance of each component in the exergy consumption of the plant it is introduced the factor f_i ([3]; see also [4]) defined as the relation between the exergy consumed by each component and the exergy consumed by the plant. The expressions of f_i for the main components of a cogeneration and power plant are summarized in Table 3.2.

With the definitions of η_{bi} and f_i it is possible to obtain an expression that relates the overall exergy efficiency of the plant, $\eta_{overall}$, with η_{bi} , and f_i .

For a cogeneration plant composed of a Rankine cycle with a back-pressure steam turbine the expression of $\eta_{b\ overall}$ is:

$$\eta_{b\ overall} = \frac{W_{st} - W_{pump} + B_q}{B_{fuel}} \quad (3.5)$$

Fig. 3.2 Scheme of a cogeneration plant



This equation can be rewritten with the use of η_i and f_i , as shown by Eq. 3.6:

$$\eta_{b \text{ overall}} = [\eta_b]_{st} f_{st} - f_{\text{pump}} + [\eta_b]_q f_q \quad (3.6)$$

In the case of a cogeneration plant composed of a gas turbine (gt is the turbine of the gas turbine) and a heat recovery steam generator the expression of $[\eta_b]_{\text{overall}}$ is:

$$\eta_{b \text{ overall}} = [\eta_b]_{gt} f_{gt} - f_{cp} + [\eta_b]_q f_q \quad (3.7)$$

Equation 3.8 presents the expression of $\eta_{b \text{ overall}}$ of a cogeneration plant, shown in Fig. 3.2 composed of a gas turbine, a heat recovery steam generator (HRSG), a back-pressure steam turbine and an absorption chiller that generates electricity, and chilled water for air conditioning purposes:

$$\eta_{b \text{ overall}} = \frac{W_{gt} - W_{cp} + W_{st} - W_{\text{pump}} + B_q}{B_{\text{fuel}}} \quad (3.8)$$

The determination of $\eta_{b \text{ overall}}$ can also be done with the use of η_i of each component of the plant.

$$\eta_{b \text{ overall}} = \left([\eta_b]_{gt} \frac{\Delta B_{gt}}{B_{\text{fuel}}} - \frac{W_{cp}}{B_{\text{fuel}}} \right) + \left([\eta_b]_{st} \frac{\Delta B_{st}}{B_{\text{fuel}}} - \frac{W_{\text{pump}}}{B_{\text{fuel}}} \right) + [\eta_b]_q \frac{B_q}{B_{\text{fuel}}} \quad (3.9)$$

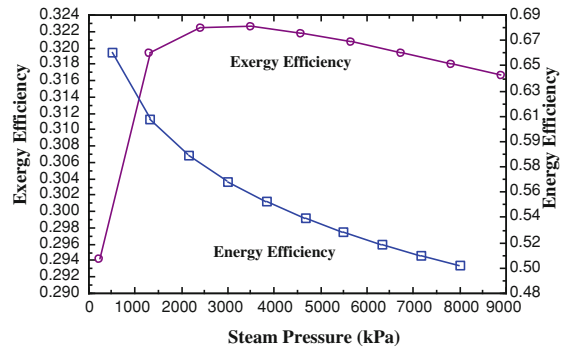
Writing $\eta_{b \text{ overall}}$ in terms of η_i and f_i of each component of the plant gives Eq. 3.10

$$\eta_{b \text{ overall}} = [\eta_b]_{gt} f_{gt} - f_{cp} + [\eta_b]_{st} f_{st} - f_{\text{pump}} + [\eta_b]_{abs} f_{abs} \quad (3.10)$$

For absorption refrigerating system η_{abs} can be given as:

$$[\eta_b]_{abs} = \text{COP} \left| \frac{\theta_{ev}}{\theta_{ge}} \right| \quad (3.11)$$

Fig. 3.3 Overall exergy and energy efficiency as a function of the steam pressure



Therefore the evaluation of the influence of each set of equipment in the overall exergy efficiency of the plant, $\eta_{b, \text{overall}}$, can be done, indicating possible ways of increasing the overall efficiency of the plant.

3.2.2 Exergy Evaluation of a Cogeneration Plant

The methodology described before is applied to the cogeneration plant based on a combined cycle, shown in Fig. 3.2. The basic operational data of this plant are:

- fuel: gas with chemical exergy of 39,150 kJ/kg;
- gas turbine pressure ratio: 14:1;
- compressor isentropic efficiency: 0.90;
- gas turbine isentropic efficiency: 0.90;
- turbine combustor outlet temperature: 1,293 K;
- gas turbine air ratio: 270 %;
- gas turbine outlet temperature: 766 K;
- steam turbine outlet pressure: 100 kPa;
- steam turbine isentropic efficiency: 0.85;
- pump isentropic efficiency: 0.70;
- transmission, generator, and mechanic efficiency: 0.95;
- substances of the absorption chiller: $\text{H}_2\text{O-LiBr}$;
- evaporation temperature of the absorption chiller: 3 °C;
- condensation temperature of the absorption chiller: 40 °C;
- weak solution concentration of the absorption chiller: 55 %;
- strong solution concentration of the absorption chiller: 60 %;
- inlet chilled water temperature: 12 °C;
- outlet chilled water temperature: 6 °C.

Figure 3.3 presents the evolution of overall exergy efficiency of the cogeneration plant as a function of the steam pressure in the heat recovery steam generator (in these calculations the transmission, generator, and mechanic efficiencies were

Table 3.3 Values of η_{bi} and f_i for the components of the cogeneration plant

Component/parameter	CC	GT	CP	HRS	ST	P	ABS
η_i	0.779	0.890	0.906	0.513	0.791	0.599	0.235
f_i	–	0.846	0.482	0.272	0.083	0.0006	0.057

CC combustion chamber, GT turbine of the gas turbine, CP air compressor, HRS heat recovery steam generator, P pump, ABS absorption chiller

considered the same for both steam and gas turbines). The performance simulation of the plant indicates a maximum value of $\eta_{b \text{ overall}}$ for a steam pressure of 3,000 kPa.

Table 3.3 summarizes the values of η_i and f_i for the components of the cogeneration plant in the condition of maximum $\eta_{b \text{ overall}}$.

In the condition of maximum overall exergy efficiency, the gas turbine converts 24.4 % of the chemical exergy of the natural gas into electricity and the steam cycle converts 6.5 %. The absorption chiller transfers 1.3 % of the chemical exergy of the natural gas to the chilled water. Therefore, the overall exergy efficiency of the plant is 32.2 %. In this operating condition the energy efficiency is 56.5 % and the ‘heat to electricity ratio’ is 0.763.

3.3 Exergy Method for Determining the Electricity Cost Formation in Combined Cycle Power Plants

3.3.1 Introduction

The needs to evaluate the cost production processes in a combined cycle power plant or cogeneration plant can be rationally conducted if the exergy of the products of the plant: electricity generated in the gas turbine, in the steam turbine, and process steam, is taken as the value basis.

This is an interesting application of thermoeconomics concepts to evaluate and allocate the cost of exergy throughout the power plant energy conversion processes, considering costs related to exergy inputs and investment in equipment. Although the concept may be applied to any combined cycle or cogeneration plant, this section describes the mathematical modeling for three-pressure heat recovery steam generator configurations and total condensation of the produced steam. It is possible to study any $n \times 1$ plant configuration (n sets of gas turbine and heat recovery steam generators associated to one steam turbine generator and condenser) with the developed model, as shown in Fig. 3.4 and Table 3.4, assuming that every train operates identically and in steady state. The presented model was conceived from a complex configuration of a real power plant, over which variations may be applied in order to adapt it to a defined configuration under study [5] such as the use of reheat, supplementary firing and partial load operation. It is also possible to undertake sensibility analysis on geometrical equipment parameters.

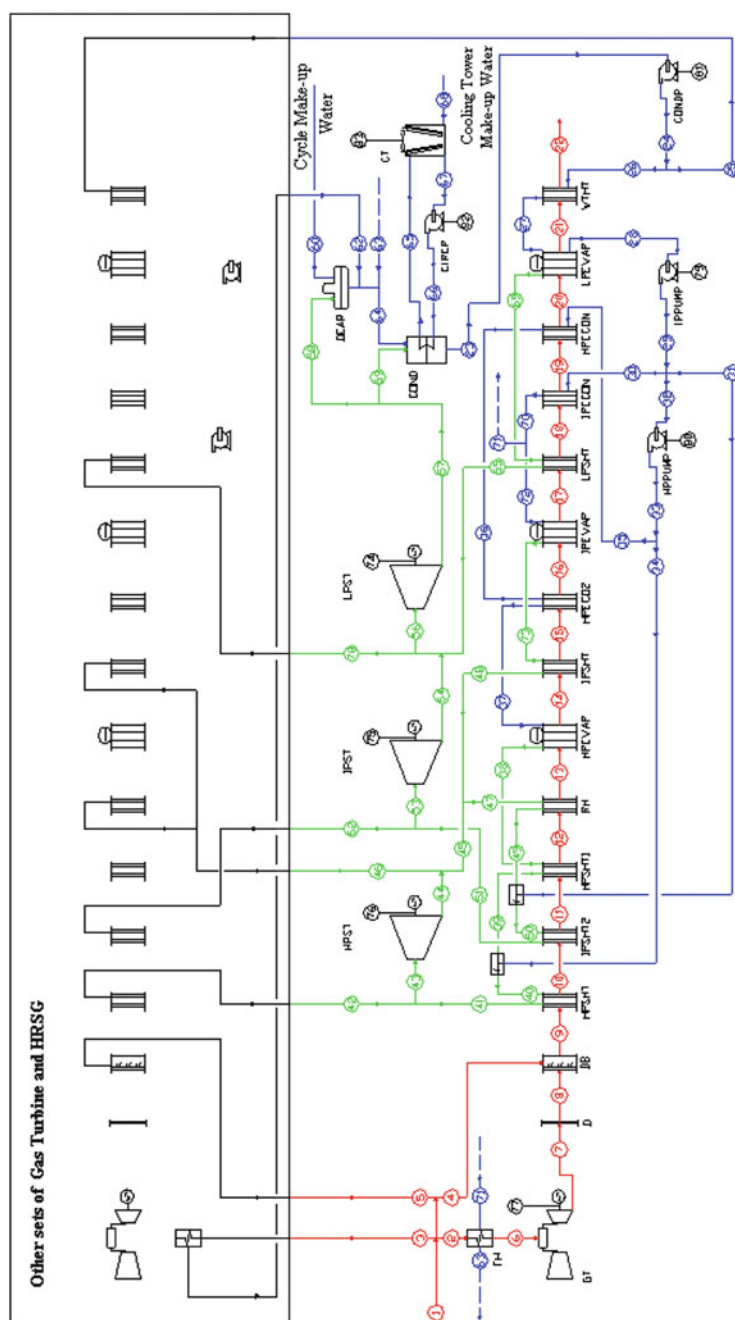


Fig. 3.4 Power plant model [5]

Table 3.4 Components nomenclature of the combined cycle shown in Fig. 3.4

Abbreviature	Component
GT	Gas turbine
D	Duct
HPPUMP	High pressure feed pump
IPPUMP	Intermediate pressure feed pump
CONDP	Condensate pump
CIRCP	Circulating pump
COND	Condenser
DEAR	Deaerator
CT	Cooling tower
<i>Heat recovery steam generator</i>	
DB	Supplementary firing module
HPSHT	High pressure superheater
IPSTH2	Intermediate pressure superheater II
HPSHT1	High pressure superheater I
RH	Reheating module
HPEVAP	High pressure evaporator
IPSHT	Intermediate pressure superheater
HPECO2	High pressure economizer II
IPEVAP	Intermediate pressure evaporator
LPSHT	Low pressure superheater
IPECON	Intermediate pressure economizer
HPECON	High pressure economizer
LPEVAP	Low pressure evaporator
WTHT	Water heater
FH	Natural gas heater
<i>Steam turbine</i>	
HPST	High pressure section
IPST	Intermediate pressure section
LPST	Low pressure section

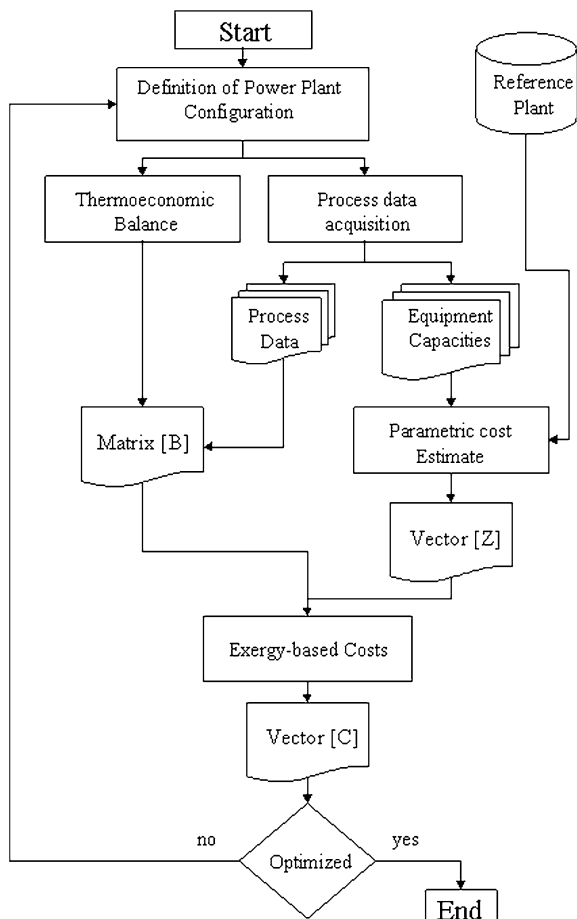
3.3.2 Method Description

The first step is to collect information on the power plant configuration under study, detailing equipment and its capacity, transport properties of each process stream, and the consumed and generated power of the plant. The data that define each stream (i.e. mass flow rate, temperature, pressure, enthalpy, entropy and, consequently, exergy) may be collected using many different sources. One usual source is a computerized process simulator.

Nevertheless, data from the digital control system of operating plants and information from engineered energy balances also provide the necessary information.

The next step comprises using the equipment capacity to estimate costs, using a parametric method, which calculates an estimated cost based on a reference biome of cost and capacity [6, 7].

Fig. 3.5 Flowchart depicting the proposed method [5]



Finally, the system of linear equations (cost balances for every component of the plant and the required cost partition criteria, for instance, for gas and steam turbines) is obtained, and from the solution of Eq. 3.12, results a vector containing exergy-based costs for each stream. From this point on, several plant characteristics may be altered, which will ultimately recalculate matrix B and vector Z of Eq. 3.12, and therefore, resulting in a new exergy-based cost vector. Improving the power plant performance depends on defining which values from this vector are to be optimized and thus seeking alterations that will produce the desired effect. Figure 3.5 illustrates the method.

$$[B]_{n \times n} [c] = [Z]_n \quad (3.12)$$

3.3.3 Cost Allocation Criteria for the Heat Recovery Steam Generator

Exhaust gases from the combustion turbine have monetary value because the steam that turns other turbines is generated from them. However, in the exhaust stack, the same gases are no longer used as far as the power plant is concerned, and for that reason cannot be assigned a value. As there is use for the exhaust gases from the combustion turbines and supplementary firing modules, these streams are assigned a cost (and the boiler stack exhaust must contain a null monetary value). Hence it is necessary to propose a criterion to distribute costs through the several modules of the heat recovery steam generator, taking into consideration the exergy of each stream and its variation.

For studying this problem, take a HRSG with n components (for instance, economizer, superheater, vaporizer, reheater), in which the reduction of the exergy flow rate of the combustion gases when flowing through a module i is ΔB_i . The overall exergy reduction in the HRSG is ΔB . If it is considered that the cost reduction of the combustion gases is a linear function of the exergy flow rate reduction in every component of the HRSG, then one can write for every module:

$$c_i = a_i c_{i-1} + b \quad (3.13)$$

where c_i is the specific exergy cost of the combustion gases at the exit of module i and c_{i-1} is the specific exergy cost of the combustion gases at the inlet of module i . The proposed relation does not imply that the combustion gases cost will have a linear reduction through the heat recovery steam generator, but only inside each module.

In order to assure that the variation of the cost in each component be proportional to the flow exergy variation, a_i is defined as [5]:

$$a_i = \left(1 - \frac{\Delta B_i}{\Delta B} \right) \quad (3.14)$$

Moreover, knowing that at the outlet of the last module the value (cost) of the gases is zero:

$$b = \left(\frac{\Delta B_n}{\Delta B} - 1 \right) c_{n-1} \quad (3.15)$$

Thus, the proposed variation law is shown in Eq. (3.16).

$$c_i = \left(1 - \frac{\Delta B_i}{\Delta B} \right) c_{i-1} + \left(\frac{\Delta B_n}{\Delta B} - 1 \right) c_{n-1} \quad (3.16)$$

This relation provides a procedure to determine the variation of the cost of combustion gases (exergy transferred and destroyed) in each module of the HRSG. This procedure is shown in Fig. 3.6.

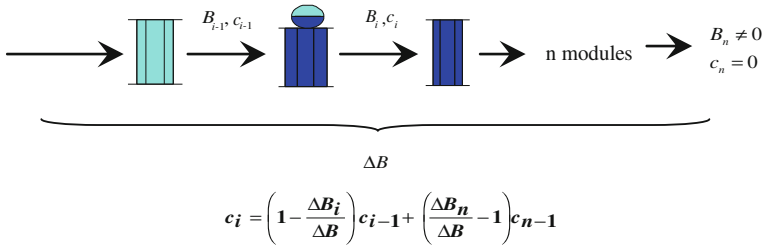


Fig. 3.6 Steam cost evaluation in the heat recovery steam generator [5]

Table 3.5 Combined cycle configurations with several gas turbines [30]

Gas turbine model	SWPC 501G	ABB GT24	SWPC 501FD	GE PG7421FA	SWPC 501DA	GE PG9171E
Gas turbine power (MW)	212.73	167.61	168.07	157.52	109.85	112.84
Power plant power (MW)	311.11	247.21	249.47	239.63	166.49	172.52
Gas turbine exergy efficiency	0.36	0.35	0.35	0.34	0.32	0.31
Power plant exergy efficiency	0.53	0.52	0.52	0.51	0.49	0.48
High pressure steam turbine power (MW)	29.02	23.94	23.91	24.25	14.82	15.82
Intermediate pressure steam turbine power (MW)	27.69	22.54	22.97	23.14	16.27	17.12
Low pressure steam turbine power (MW)	41.66	33.11	34.52	34.72	25.55	26.75
Installation cost ^a (US\$/kW)	324.67	314.05	336.39	348.70	385.16	382.63
Gas turbine electricity cost (US\$/MWh)	17.60	17.18	17.72	17.59	18.23	18.51
High pressure steam turbine electricity cost (US\$/MWh)	41.86	42.26	42.68	42.58	47.61	47.07
Intermediate pressure steam turbine electricity cost (US\$/MWh)	45.17	45.42	45.88	45.82	50.84	50.23
Low pressure steam turbine electricity cost (US\$/MWh)	61.47	61.50	62.52	62.48	66.45	66.01
Average electricity cost (US\$/MWh)	28.20	28.12	28.90	29.35	31.43	31.64

^a Installation costs presented are referred to power island only. Power island comprises gas turbine, steam turbine, steam generator, condenser, condensing, and steam generator feeding pumps [31]

3.3.4 Results

Table 3.5 shows results of comparisons made using 1×1 power plants using several combustion turbines technology, as a first application of the method. The configuration of the heat recovery boiler is equal for every simulation, and comprising three pressures and three modules in each pressure level, and no reheating.

Table 3.6 $N \times 1$ configurations study [30]

Configuration	1×1	2×1	3×1
Gas turbine power (MW)	167.61	167.61	167.61
Power plant capacity (MW)	247.21	490.12	567.96
Gas turbine exergy efficiency	0.35	0.35	0.35
Power plant exergy efficiency	0.52	0.52	0.52
High pressure steam turbine power (MW)	23.94	49.28	74.63
Intermediate pressure steam turbine power (MW)	22.54	44.98	67.42
Low pressure steam turbine power (MW)	33.11	66.05	98.99
Installation cost (power island) (US\$/kW)	314.05	257.17	221.92
Electricity cost—Gas turbine (US\$/MWh)	17.18	17.17	17.17
Electricity cost—High pressure steam turbine (US\$/MWh)	42.26	38.84	37.51
Electricity cost—Intermediate pressure steam turbine (US\$/MWh)	45.42	42.69	41.65
Electricity cost—Low pressure steam turbine	61.50	47.22	43.11
Average electricity cost (US\$/MWh)	28.12	25.65	24.88

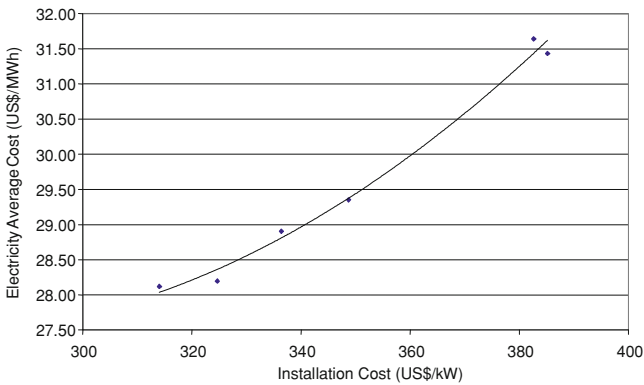


Fig. 3.7 Installation cost study [5]

It was allowed to the simulator [8] to adjust the modules within a range of geometrical characteristics to obtain best results for each configuration.

The electricity production costs were determined considering interest rate of 17 % per year, 20 years as the capital recovery period and a load factor of 92 %.

By analyzing Table 3.5 and Fig. 3.7, one can notice the relation between exergy efficiency and the average cost of electricity. The comparison between a plant based on ABB GT24 machine and another based on a SWPC 501G shows that the installation cost may sometimes compensate a lower efficiency.

A deeper analysis of Table 3.5 allows the study of the composition of the average cost as a function of the costs calculated in each generator. The lower value is related to the combustion turbine generator for all cases. Hence, the addition of more combustion turbines in 2×1 or 3×1 configurations results in lower average costs. Table 3.6 and Fig. 3.8 show results obtained by varying the number of ABB GT24 machines in the power plant.

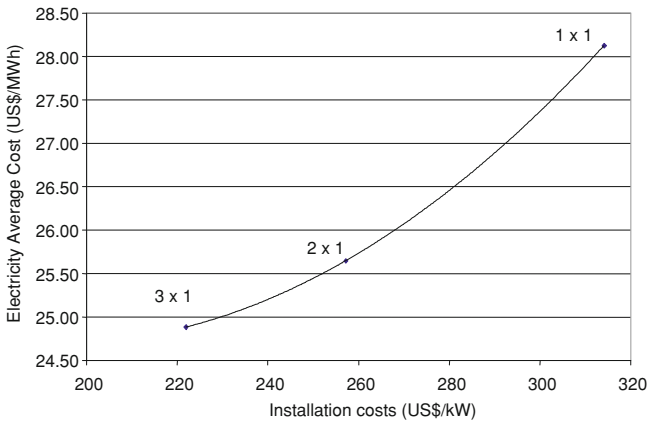


Fig. 3.8 ' $n \times 1$ ' configuration study [5]

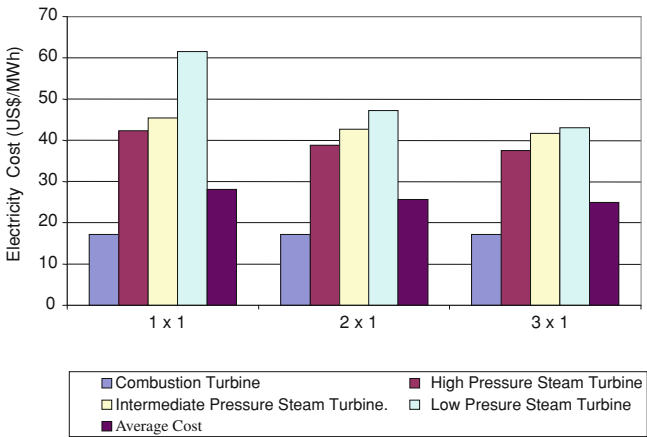


Fig. 3.9 Electricity cost composition [5]

By analyzing Table 3.6 and Fig. 3.8, it can be observed that adding more combustion turbines reduces the average cost. The installation costs also decreased, indicating a scale gain. Figure 3.9 depicts that the average costs are much influenced by the low pressure steam turbine in the 1×1 configuration. The other configurations show more equalized costs; however, the electricity generation in this section is the highest in considering all steam turbine sections. To solve this problem it is necessary either to decrease its production or to increase production in other sections, in such a way that the average cost will be reduced. Table 3.7 presents results obtained with three optimization studies of a 2×1 ABB GT24 power plant.

The first study shows results for the same configuration studied before. In Study 2, reheat modules were added, along with other high and intermediate pressure modules. The efficiency increase can be observed, but the addition of a reheat section

Table 3.7 Cycle optimization [30]

Study	1	2	3
Gas turbine power (MW)	167.61	167.48	167.48
Power plant capacity (MW)	490.12	505.81	512.01
Gas turbine exergy efficiency	0.35	0.36	0.36
Power plant efficiency	0.52	0.54	0.55
High pressure steam turbine power (MW)	49.28	41.15	41.15
Intermediate pressure steam turbine power (MW)	44.98	60.91	60.95
Low pressure steam turbine power (MW)	66.05	73.79	79.90
Installation cost (power island) (US\$/kW)	257.17	264.18	260.98
Electricity cost—Gas turbine (US\$/MWh)	17.17	17.28	17.28
Electricity cost—High pressure steam turbine (US\$/MWh)	38.84	45.37	40.69
Electricity cost—Intermediate pressure steam turbine (US\$/MWh)	42.69	30.97	28.45
Electricity cost—Low pressure steam turbine	47.22	45.73	36.01
Average electricity cost (US\$/MWh)	25.65	25.21	23.41

rearranged the steam and power generation inside, producing new results. The average cost was reduced; however, the low pressure section continues to push its value upwards.

Study 3 was obtained taking the condenser pressure from 0.10 to 0.06 bar. Consequently, the destruction of exergy in this component was reduced, which reduced also the exergy-based costs of the condensate and the boiler feed water. Hence, the steam was generated at a lower cost, which pulled the overall costs downwards, especially in the low pressure section, which had its power production increased. In this sense, the combined result is a lower average electricity cost. Table 3.8 shows pinch points of evaporators and approach temperatures (temperature difference between gas inlet and steam or liquid outlet) of other heat exchangers of the heat recovery steam generators.

Table 3.9 summarizes the data of every section of the optimized 2×1 ABB GT24 power plant (shown in Fig. 3.4). Data of Table 3.9 indicate how is the electricity cost formation process, as well as the composition of the average electricity cost.

Figure 3.10 depicts the effect of the proposed law of variation over the exergy-based cost of the exhaust gases (see also Fig. 3.4). It can be observed that the stack exhaust carried no monetary value, and the cost is distributed to each module according to the exergy it captures. Hence the high pressure sections, which use more of the exergy of the gas exhaust stream, received larger portion of costs.

Aiming to demonstrate the applicability of the method to sensitivity analysis, Figs. 3.11 and 3.12 are presented. Both based on a 1×1 SWPC 501FD power plant.

Figure 3.11 shows the response of the electricity exergy-based cost and efficiency to a variation in the condenser pressure. As a lower condenser pressure implies in larger heat exchanger areas, pumps and cooling towers, the method allows the capital costs to vary to capture these changes, and produce results according to the heat balance modifications. Figure 3.12 depicts the behavior of the exergy-based cost according to the load condition of the power plant. Partial

Table 3.8 Heat recovery steam generators pinch points and approach temperatures [30]

	Study 1 (°C)	Study 2 and 3 (°C)
HPSHT	88	88
IPSTH2	^a	32
HPSHT1	^a	130
RH	^a	31
HPEVAP	10	10
IPSHT	30	20
HPECO2	50	15
IPEVAP	10	10
LPSHT	10	16
IPECON	35	28
HPECON	^a	13
LPEVAP	10	10
WTHT	40	29

^a Nonoperating

load conditions produce naturally less efficient results, a consequence which can be captured by the method when allocating cost according to exergy destruction, thus resulting in higher costs.

The last set of results comprises the study on supplementary firing. The base power plant model for this study is a 2×1 SPWC 501F, which generates 590 MW using its full supplementary firing capacity, which corresponds to its design condition.

The fuel burnt in the heat recovery boilers is decreased until it is completely turned off, in which case the power plant produces approximately 500 MW. The installation cost is kept constant throughout the study in order to more accurately reflect the load variations and investment in excess capacity. Figures 3.13 and 3.14 present the variation of the exergy-based cost of electricity and according both to power generation and to plant efficiency.

It can be observed that the efficiency decreases with the increase of power generation, which is to be expected since the supplementary firing causes this effect on the overall cycle efficiency. However, the exergy-based cost of electricity generated finds a local minimum value, which can be interpreted as the balance between the loss in terms of efficiency and its compensation in capital cost utilization, since operating the supplementary firing in less than 100 % capacity implies using less capacity than the installed.

3.3.5 Comments on the Method Application

With the described method is possible to analyse the composition of the electricity costs in a variety of combined cycle power plants configurations. The parametric cost estimation allows the method to vary equipment costs accordingly to the capacity of the equipment used, providing parameters for a cost–benefit analysis.

Table 3.9 Characteristics of the 2×1 optimized configuration [30]

	m (kg/s)	P (bar)	T (°C)	b (kJ/kg)	B (kW)	c_b (US\$/MWh)	c_m (US\$/t)
1	17.98	34.47	25.00	52324.49	940590.72	10.08	146.51
2	8.99	34.47	25.00	52324.49	470295.33	10.08	146.51
3	8.99	34.47	25.00	52324.49	470295.33	10.08	146.51
4	—	34.47	25.00	52324.49	—	10.08	146.51
5	—	34.47	25.00	52324.49	—	10.08	146.51
6	8.99	34.47	141.12	52379.69	470791.47	10.44	151.90
7	373.29	1.03	654.59	675.00	251971.85	10.44	1.96
8	373.29	1.01	654.59	673.09	251258.76	10.44	1.95
9	373.29	1.01	654.59	673.09	251258.76	10.44	1.95
10	373.29	1.01	628.10	634.06	236691.52	9.36	1.65
11	373.29	1.01	611.21	609.44	227500.14	8.64	1.46
12	373.29	1.01	538.78	506.34	189013.94	7.20	1.01
13	373.29	1.01	489.93	439.33	163998.05	6.12	0.75
14	373.29	1.01	341.04	251.13	93745.47	3.96	0.28
15	373.29	1.01	337.16	246.62	92061.00	3.60	0.25
16	373.29	1.01	271.92	174.45	65119.93	2.88	0.14
17	373.29	1.01	242.30	144.28	53860.50	2.16	0.09
18	373.29	1.01	240.40	142.42	53162.94	1.80	0.07
19	373.29	1.01	233.39	135.57	50607.66	1.44	0.05
20	373.29	1.01	193.21	98.59	36803.79	1.08	0.03
21	373.29	1.01	156.63	68.62	25614.39	0.36	0.01
22	373.29	1.01	91.00	25.83	9642.43	—	—
23	132.25	0.06	33.96	8.66	1144.66	2180.77	5.24
24	132.25	4.55	34.07	9.15	1210.20	2067.70	5.25
25	66.13	4.55	34.07	9.15	605.10	2067.70	5.25
26	66.13	4.55	34.07	9.15	605.10	2067.70	5.25
27	66.13	4.35	127.75	97.50	6447.59	203.10	5.50
28	61.74	4.35	146.63	124.51	7687.61	119.55	4.13
29	61.74	29.38	147.22	127.71	7885.26	119.91	4.25
30	9.91	29.38	147.22	127.71	1265.05	119.91	4.25
31	—	29.38	147.22	127.71	—	119.91	4.25
32	51.84	29.38	147.22	127.71	6620.21	119.91	4.25
33	51.84	130.55	149.16	140.00	7257.54	114.51	4.45
34	—	130.55	149.16	140.00	—	114.51	4.45
35	51.84	130.55	149.16	140.00	7257.54	114.51	4.45
36	51.84	130.35	220.52	266.18	13798.32	66.26	4.90
37	51.84	130.35	322.30	528.39	27390.56	40.69	5.97
38	51.32	130.35	331.04	1694.05	86937.83	20.89	9.83
39	51.32	130.35	482.00	1547.03	79393.01	31.33	13.46
40	51.32	130.35	482.00	1547.03	79393.01	31.33	13.46
41	51.32	125.14	566.80	1692.80	86873.66	33.13	15.57
42	51.32	125.14	566.80	1692.80	86873.66	33.13	15.57
43	102.64	125.14	566.80	1692.80	173747.32	33.13	15.57
44	102.64	28.01	347.66	1267.41	130086.36	33.13	11.66
45	51.32	28.01	347.66	1267.41	65043.18	33.13	11.66

(continued)

Table 3.9 (continued)

	m (kg/s)	P (bar)	T (°C)	b (kJ/kg)	B (kW)	c_b (US\$/MWh)	c_m (US\$/t)
46	51.32	28.01	347.66	1267.41	65043.18	33.13	11.66
47	57.69	28.01	344.68	1263.53	72898.13	33.13	11.62
48	6.37	28.01	321.18	1232.78	7858.11	34.57	11.83
49	57.69	26.89	507.74	1480.81	85433.89	32.77	13.48
50	57.69	26.89	507.74	1480.81	85433.89	32.77	13.48
51	57.69	26.89	566.00	1566.85	90397.86	33.85	14.73
52	57.69	26.89	566.00	1566.85	90397.86	33.85	14.73
53	115.39	26.89	566.00	1566.85	180795.72	33.85	14.73
54	115.39	4.17	305.83	1200.13	138480.23	33.85	11.28
55	4.38	4.17	226.54	931.88	4084.17	117.39	30.38
56	124.15	4.17	300.21	1006.58	124969.78	41.05	11.47
57	124.15	0.06	36.18	512.62	63644.10	41.05	5.84
58	0.04	0.06	36.18	276.73	12.23	41.05	3.15
59	124.11	0.06	36.18	276.73	34344.85	41.05	3.15
60	1.17	1.03	15.56	2.42	2.82	3075.26	2.06
61	1.21	0.06	36.18	9.71	11.75	792.58	2.14
62	3.47	29.18	44.21	16.89	58.56	76.34	0.36
63	3.47	29.18	44.21	16.89	58.56	76.34	0.36
64	8.14	0.06	36.18	39.89	324.85	56.18	0.62
65	6788.52	2.20	34.83	9.27	62939.88	2180.77	5.61
66	6788.52	2.20	24.83	5.18	35139.54	3932.66	5.65
67	6788.52	1.01	24.83	5.06	34318.10	4025.93	5.65
68	133.10	2.00	15.00	2.39	318.40	1875.05	1.25
69	4.38	4.35	146.63	866.04	3795.64	119.55	28.75
70	9.91	29.18	212.30	241.50	2392.19	76.34	5.12
71	3.47	29.18	212.30	241.50	837.27	76.34	5.12
72	6.44	29.18	212.30	241.50	1554.92	76.34	5.12
73	6.37	29.18	232.30	1110.13	7076.34	31.69	9.77
74					79902.97	36.01	—
75					60948.65	28.45	—
76					41147.11	40.69	—
77					167483.90	17.28	—
78	4.38	4.17	226.54	931.88	4084.17	117.39	30.38
79					252.80	23.41	—
80					763.72	23.41	—
81					113.63	23.41	—
82					954.25	23.41	—
83					1744.16	23.41	—

The application of cost balances showed its benefits in terms of process analysis, allowing a detailed study of each stream that comprises the power plant. The proposed law of variation on the exergy-based cost of the exhaust gases aided to identify the costs, which affect significantly the composition of the electricity average cost.

Fig. 3.10 Effect of the combustion gases cost law variation [5]

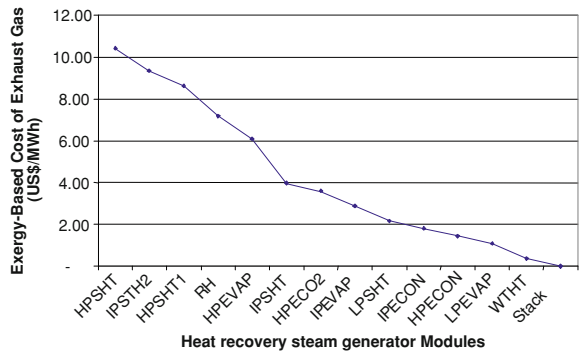


Fig. 3.11 Sensitivity analysis: condenser pressure [5]

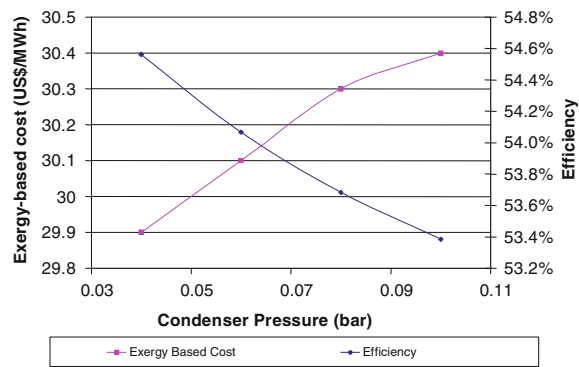
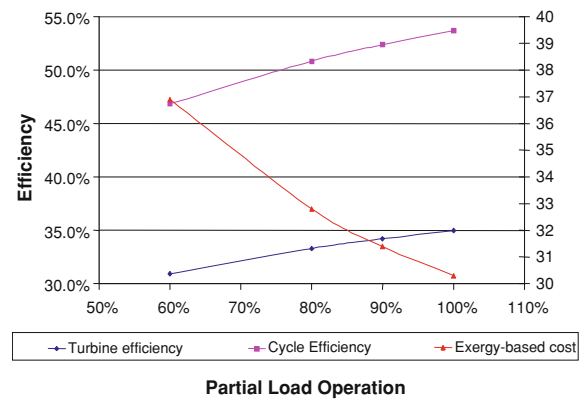


Fig. 3.12 Sensitivity analysis: partial load operation [5]



Another advantage of the method is providing data for a cost–benefit analysis, combining thermoeconomics, and parametric cost estimation. Investment decisions may be based on parameters provided by the method, in terms of equipment sizing and reheat application. As seen in the supplementary firing cases, similar analysis may provide data for peaking plant operation.

Fig. 3.13 Cost variation according to generated power [5]

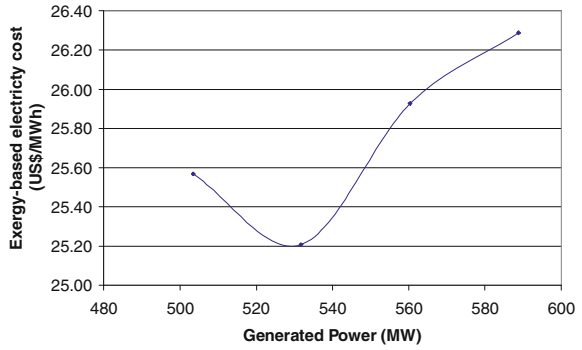
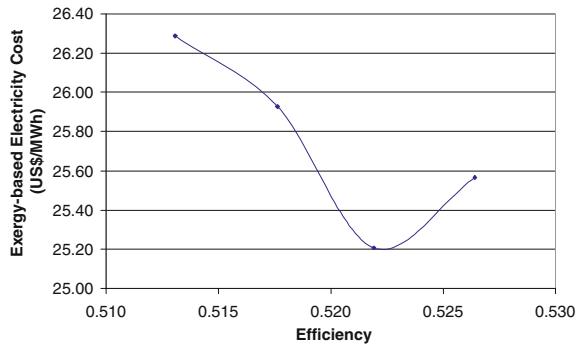


Fig. 3.14 Cost variation according to efficiency [5]



Another possible outcome of using the described method is evaluating the impact of emissions-trading schemes in the cost of electricity. Assuming that a monetary value can be assigned to the exhaust stack gases, the solution of the whole system of equations will then reallocate costs to accurately reflect the costs of emissions.

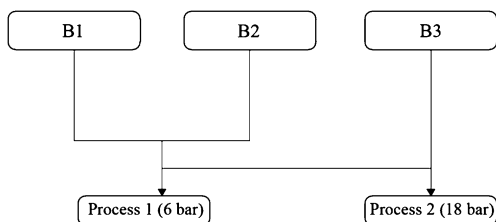
Additionally, it must be pointed out that the methodology will be also useful in the determination of the steam production cost in cogeneration plants.

3.4 Exergy and Thermoeconomic Evaluation of Cogeneration Plants for a Chemical Industry

3.4.1 Introduction

The projected increase of the natural gas consumption in countries like Brazil has motivated several substitution studies in industrial processes in order to analyze the feasibility of the use of this fuel in utilities plants. Together with these studies, the possibility of adapting these plants to be converted into cogeneration plants is also considered.

Fig. 3.15 Scheme of the steam distribution line [11]



In the Brazilian Chemical Industrial Sector, 37 % of the energy consumption in 1998 corresponded to steam generation in boilers for heating purposes, with residual fuel oil accounting for 53 % of this consumption [9]. In these industries the average heat-to-power ratio is 1.88 [10].

The study described next presents a thermo-economic analysis of three cogeneration systems designed to be used in a chemical plant that intends to increase its steam generation capacity and substitute fuel oil by natural gas, to generate electricity and steam to its processes.

The use of exergy and thermo-economic analysis provides a rational way to evaluate the production costs of these utilities for different technological options, as well as, in different operating conditions.

In this way, three cogeneration systems: a steam cycle with condensation–extraction steam turbine, a gas turbine-based system, and a combined cycle based system, are analyzed in two operating scenarios: in the first one the systems generate steam (10 t/h at 18 bar and 30 t/h at 6 bar) and electricity for the plant (5 MW) and in the second one the systems generate steam (10 t/h at 18 bar and 30 t/h at 6 bar), electricity for the plant (5 MW) and export electricity (12 MW).

3.4.2 Steam and Electricity Demands

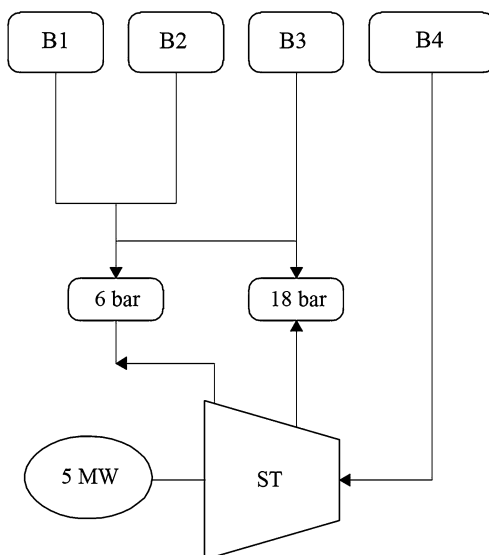
The utilities plant of the chemical industry is made up of three steam boilers (B1, B2, and B3), generating steam at two pressure levels, 6 bar (to feed process 2) and 18 bar (to feed process 1). The higher pressure line is connected to the lower pressure one, as shown in Fig. 3.15. According to the Energy Department of the industry, the average monthly consumption of process steam and electricity [11] are:

- electricity: 3,886 MWh
- process steam: 14,942 t

The cost of each one of the utilities considered by the industry [11] is:

- electricity: 68.00 US\$/MWh
- process steam: 17.40 US\$/t

Fig. 3.16 Simplified flow sheet of the utilities plant with condensation–extraction steam turbine [11]



3.4.3 Cogeneration Systems

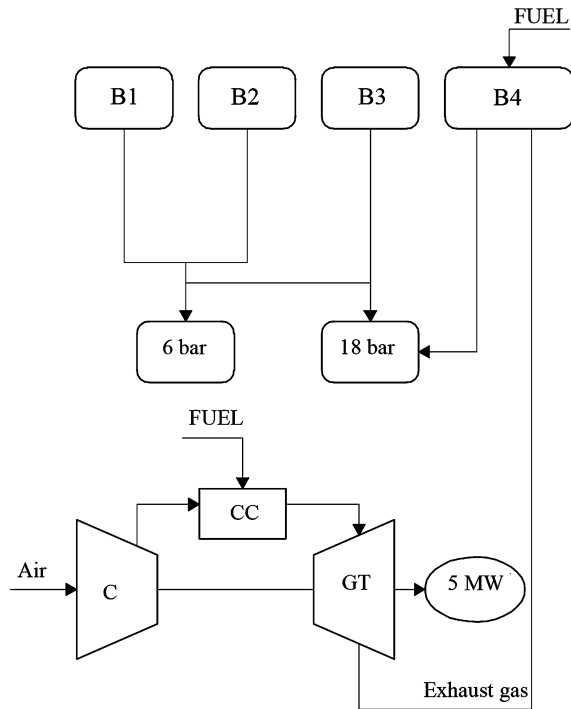
As mentioned before, the considered cogeneration systems are: a steam cycle with condensation–extraction steam turbine, a gas turbine based system, and a combined cycle based system [11].

The steam turbine based system is composed of a condensation–extraction steam turbine and a high pressure steam generator (B4). The electricity generation capacity is 5 MW. Figure 3.16 shows a simplified flow sheet of this configuration. Steam is generated in the boiler B4 at a pressure of 42 bar and 573 K. This steam is sent to the condensation–extraction steam turbine, where 10 t/h of steam are extracted at 18 bar (process 1) and 30 t/h extracted are at 6 bar (process 2).

The gas turbine-based cycle is made up of a gas turbine of the same capacity as the steam turbine (the combustion chamber outlet temperature is 1,295 K) and a waste heat boiler (B4) that can produce 16.67 t/h of steam at 20 bar. This waste heat boiler must operate with supplementary consumption of natural gas to attain the plant steam demand. This configuration is shown in Fig. 3.17.

Figure 3.18 shows the combined cycle-based cogeneration system. In this configuration the gas turbine-based system is coupled with a steam cycle with a waste heat boiler. The extraction steam conditions and flow rates are the same of the steam turbine-based system. In this system the electricity generation capacity is fixed to 6.3 MW because the steam-based system must produce 40 t/h of steam to supply the processes demand, implying that the industry is able to export 1.3 MW of electricity. This means that the waste heat boiler must consume supplementary fuel to increase the steam production. In Fig. 3.18 it is indicated that the gas

Fig. 3.17 Simplified flow sheet of the utilities plant with the gas turbine-based system [11]



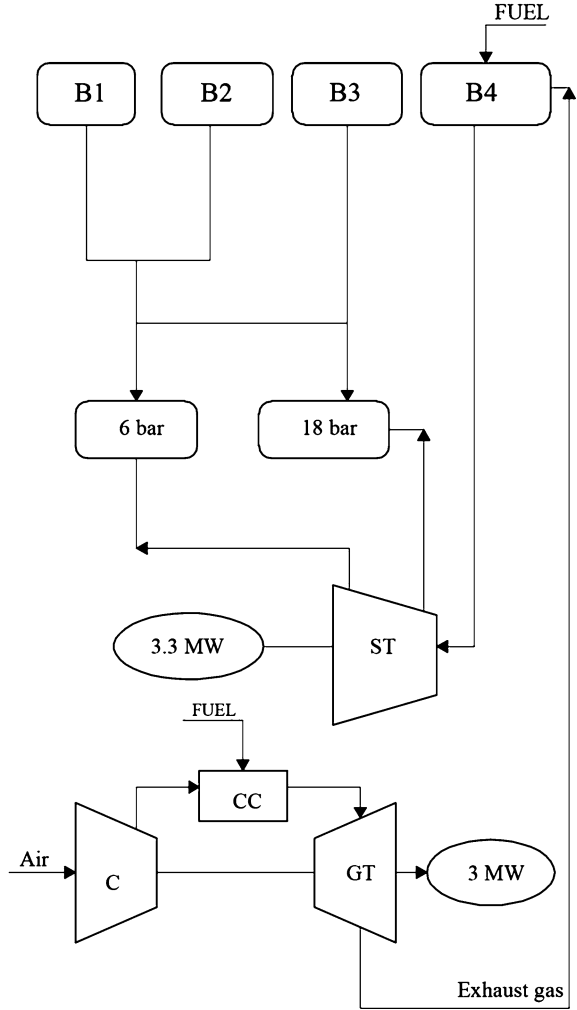
turbine generates 3.0 MW and the steam turbine generates 3.3 MW. This power distribution is obtained by the simulation of the whole system [11].

3.4.4 Exergy Analysis of the Cogeneration Systems

The methodology described in Sect. 3.2 of this chapter (see Table 3.1, Eqs. 3.5–3.8) is applied to analyze the three cogeneration systems, considering the following basic data of each plant:

- thermodynamic reference state: $T_o = 298 \text{ K}$; $P_o = 1 \text{ bar}$
- fuel: natural gas (lower heating value = 48,160 kJ/kg)
- gas turbine pressure ratio: 10:1
- isentropic efficiency of the air compressor and gas turbine: 90 %
- thermal efficiency of the gas turbine combustor: 100 %
- gas turbine combustor outlet temperature: 1,295 K
- gas turbine excess air ratio: 275 %
- exhaust gas turbine temperature: 788 K
- steam generation pressure: 42 bar
- steam generation temperature: 573 K
- steam condensation pressure: 0.05 bar

Fig. 3.18 Simplified flow sheet of steam distribution line including the proposed combined cycle [11]



- thermal efficiency of the conventional boiler: 90 %
- thermal efficiency of the heat recovery steam generator: 80 %
- isentropic efficiency of the steam turbine stages: 85 %
- isentropic efficiency of the pumps: 80 %
- mechanical, generator, and transmission efficiency: 95 %
- steam pressure of process 1: 18 bar
- average steam temperature of process 1: 450 K
- steam pressure of process 2: 6 bar
- average steam temperature of process 2: 403 K

The performance behavior of each system was simulated by means of models developed with the aid of the software EES[®] [12]. Tables 3.10, 3.11, and 3.12

Table 3.10 Parameter f_i and η_{bi} of the components of the steam turbine-based cogeneration system shown in Fig. 3.16 ($W = 5$ MW) [11]

Component	f_i	η_{bi}
Boiler	1.00	0.37
Turbine	0.17	0.75
Process 1	0.05	0.89
Process 2	0.13	0.84
Pumps	0.00	0.75
Deaerator	0.04	0.97
Preheater	0.03	0.97

present the values of f_i and η_{bi} for each component of the three cogeneration systems.

In Table 3.10 it can be seen that the steam turbine and process 2 are the main consumers of fuel exergy. Boiler 4 is the component with the lowest value of η_{bi} due to the heat transfer and combustion irreversibility that take place in this component during the processes of energy conversion.

Table 3.11 summarizes the results obtained with the gas turbine-based cogeneration system. It is interesting to notice the changes in the values of f_i and η_{bi} of the waste heat boiler when it operates with supplementary use of natural gas, indicating a reduction of the exergy efficiency in the steam generation process.

Table 3.12 shows the results of the combined cycle-based system for the second operating scenario ($W = 17$ MW). As the steam turbine must produce 5 MW, the heat recovery steam generator needs to burn natural gas. As a consequence of this operating condition, the value of the exergy efficiency of the waste heat boiler is similar to the values of this component obtained for the steam and gas turbine-based systems.

Table 3.13 presents the overall energy and exergy efficiencies of the cogeneration systems for both operating scenarios. In the first scenario, the combined cycle-based system is the most efficient one based on an exergy analysis. In the second operating scenario, the gas turbine-based system is the most efficient system, in energy and exergy analysis, because it is not necessary to burn supplementary fuel in the waste heat boiler to attain the steam demand in the processes.

3.4.5 Thermoeconomic Analysis of the Cogeneration Systems

In a multi-product plant the determination of the production cost of each utility can be done by the application of utilities cost balances and cost partition methods to the components of the plant. As stated in Chap. 2, in a thermomechanical conversion plant cost balances based on exergy balances provide a rational way to obtain the production costs of the utilities [13].

By applying the cost balance equation to the steam turbine, shown in Fig. 3.16, gives (C_{turb} = steam turbine cost rate, W_e = electric power, hp = high pressure,

Table 3.11 Parameter f_i and η_{bi} of the components of the gas turbine based cogeneration system with and without supplementary burning (sb) of fuel [11]

Component	f_i^a	f_{sbi}^b	η_{bi}^a	$\eta_{b(sbi)}^b$
Air compressor	0.40	0.21	0.90	0.90
Combustion chamber	1.36	0.73	0.75	0.75
Turbine	0.74	0.40	0.91	0.91
Waste heat boiler	0.26	0.60	0.51	0.40
Process 1	0.03	0.06	0.89	0.89
Process 2	0.08	0.15	0.84	0.84

^a $W = 17$ MW^b $W = 5$ MW**Table 3.12** Parameter f_i and η_{bi} of the components of the combined cycle based cogeneration system ($W = 17$ MW) [11]

Component	f_i	η_{bi}
Air compressor	0.25	0.90
Combustion chamber	0.84	0.79
Gas turbine	0.49	0.91
Waste heat boiler	0.56	0.38
Steam turbine	0.10	0.79
Process 1	0.03	0.89
Process 2	0.08	0.84
Pumps	0.00	0.74
Deaerator	0.02	0.97
Preheater	0.02	0.98

Table 3.13 Overall energy (η_{eG}) and exergy efficiencies (η_{bG}) of the proposed cogeneration systems for two operating conditions ($W = 5$ MW/ $W = 17$ MW) [11]

System configuration	η_{eG}	η_{bG}
Gas turbine	0.80/0.63	0.31/0.36
Steam turbine	0.72/0.43	0.29/0.25
Combined cycle	0.76 ^a /0.60	0.32 ^a /0.35

^a $W = 6.3$ MW

e = electricity, $p1$ = steam demanded by process 1, $p2$ = steam demanded by process 2, cd = condenser):

$$c_e W_e + c_{p1} \Delta B_{p1} + c_{p2} \Delta B_{p2} + c_{cd} B_c = c_{hp} B_{hp} + C_{turb} \quad (3.17)$$

In this equation B_{hp} , W_e , ΔB_{p1} and ΔB_p are determined by the exergy analysis of the plant. C_{turb} is known and c_{hp} is obtained by applying the cost balance to boiler 4, where there is only one product (high pressure steam).

To determine the values of c_e , c_{p1} , and c_{p2} it is necessary to consider a cost partition criterion. In this study, the extraction and the equality criteria are used in steam and gas turbines, giving the auxiliary relations shown in Table 3.14.

Table 3.14 Auxiliary relations

Cost partition method	Steam turbine	Gas turbine
Extraction	$c_{hp} = c_{p1} = c_{p2} = c_{cd}$	$c_{gas} = c_{eg}$
Equality	$c_e = c_{p1} = c_{p2} = c_{cd}$	$c_e = c_{eg}$

The compared thermoeconomic analysis of the three cogeneration systems shown in Figs. 3.15, 3.16, and 3.17 is obtained based on the following parameters (the components costs were evaluated for a power generation of 5 MW):

- natural gas cost: 10.40 US\$/MWh (3 US\$/MBtu);
- capital recovery period: 10 years;
- interest rate: 12 % per annum;
- load factor: 0.80;
- time factor 0.85;
- condensation–extraction steam turbine cost: US\$2,500,000;
- conventional boiler cost: US\$1,650,000;
- gas turbine cost: US\$1,950,000;
- waste heat boiler cost: US\$1,100,000;
- auxiliary equipment cost: US\$277,000;
- annual operational and maintenance cost: 10 % of the investment cost;
- inflation is not considered.

The equipment cost rate is evaluated according to Eq. 3.18:

$$C_{equip i} = C_{0i}[(n/(1 - (1 + n)^{-T}) + f_{om})/(3600 N_h f_i f_l)] \quad (3.18)$$

Table 3.15 presents the specific production costs of process steam (US\$/t) and electricity (US\$/MWh), for the three cogeneration systems and using the equality and extraction cost partition methods.

For the combined cycle-based system, the average electricity cost calculated from the values of the electricity cost of the steam and gas turbines is presented. It is interesting to notice that, for this system, the electricity generated by the gas turbine is less expensive than the electricity generated by the steam turbine, in both cost partition methods (28.66 US\$/MWh against 52.21 US\$/MWh and 46.80 US\$/MWh against 72.17 US\$/MWh).

Values of Table 3.15 indicate that only the electricity cost of the steam turbine-based system, using the extraction method, is higher than the electricity price paid by the industry (68.00 US\$/MWh). In this table it is important to verify that all obtained costs of process steam are lower than the original value considered by the industry.

Another interesting scenario to compare the performance of the systems is the one in which all the three systems are capable to generate more electricity than needed in the industry. In this scenario the company will be able to export electricity to other industries or to the electricity grid. The thermoeconomic analysis is done, in this case, for an electricity generation capacity of 17 MW [10]. In this scenario the gas turbine-based system operates without supplementary use of fuel in the heat recovery steam generator because of the higher capacity of the gas

Table 3.15 Specific production costs of electricity and process steam (mass weighted average value of the two processes) [11]

Method	Equality		Extraction	
	Electricity (US\$/MWh)	Steam (US\$/t)	Electricity (US\$/MWh)	Steam (US\$/t)
System configuration				
Steam turbine	50.26	10.78	70.92	7.73
Gas turbine	29.06	9.70	48.02	7.25
Combined ^a Cycle	40.82	11.26	59.90	7.83

^a $W = 6.3$ MW**Table 3.16** Specific production costs of electricity and process steam (mass weighted average value of the two processes) considering production of 17 MW [11]

Method	Equality		Extraction	
	Electricity (US\$/MWh)	Steam (US\$/t)	Electricity (US\$/MWh)	Steam (US\$/t)
System configuration				
Steam turbine	59.25	12.71	67.98	8.33
Gas turbine	26.01	12.97	41.88	5.99
Combined cycle	35.75	13.40	47.24	7.48

turbine. The combined cycle-based system needs to burn supplementary fuel in the heat recovery steam generator to attain the steam demand of the processes (in this system the gas turbine generates 12 MW and the steam turbine generates 5 MW).

The new components cost are determined by using some relations presented by Boehm [7] and information given by equipment manufacturers.

Table 3.16 shows the new values of electricity and process steam production costs. The electricity costs obtained for the gas turbine-based system and for the combined cycle-based system are lower than those calculated for the same type of systems in the first scenario. As observed in the first scenario, the steam turbine-based system gives the higher electricity production costs.

3.4.6 Discussion of the Obtained Results

The results given by the thermoeconomic analysis indicate that the three cogeneration systems have attractive performance and production costs of the utilities, which are competitive with the prices paid today by the industry. During the capital recovery period, the system that presents the lowest overall cost rate is the gas turbine one, in both operating scenarios.

Besides the results given by the thermoeconomic analysis some other aspects must be considered to choose the best cogeneration system such as operational flexibility and reliability of the equipment, and environmental impacts from cogeneration systems operation.

3.5 Exergy and Thermo-economic Evaluation of Utilities Plants for a Dairy Industry

3.5.1 Introduction

The evaluation of cogeneration systems described in this chapter was conducted for the Colombian industrial sector scenario in order to provide a rational utilization of fossil fuels and reduction of electricity demand from the National Interconnected System of the country (SIN). The use of cogeneration systems in the Colombian industrial sector is important because this sector is the major consumer of natural gas, oil, and coal and the second major consumer of electricity in the country.

In the industrial sector, food industry is the major energy consumer. It also has the greater cogeneration potential. Within the food industrial sector, the dairy industry is a very interesting one because it demands various utilities and has a great variety of products and processes. Colombia has important natural gas reserves and the cogeneration systems could optimize its use. In addition to this fact, the substitution of the fuel oil used in the dairy industry by natural gas could bring environmental advantages [14].

The dairy industry, used as a model for the analysis in this study, produces milk, yogurt, cheese, oats, fats, and desserts of different types. The whey, that is a by-product of the processes, is used in the production of some drinks and in the feeding of pigs that are sold alive.

The utilities demand curves of the whole plant were constructed based on the demands of the main equipment and on their hourly tendency. In order to do that, it was made a survey of the processes that take place in every section of the plant and an inventory of the equipment operation in each process. The required utilities were identified and the thermal loads and mass flow rates were all calculated in an hourly basis [14].

3.5.2 Utilities Plant Description

This dairy industry demands electricity, steam, chilled water, compressed air, and potable water (see Figs. 3.19, 3.20).

The energy consumption and demand conditions and the means of production of the utilities for this plant are as follows:

- The plant uses electricity to operate pumps, stirring rods, beaters, mills, slicing machines, and packing machines, heating systems, fans and compressors, among others. The average power demand is 2.89 MW with a peak power demand of 3.16 MW (see Fig. 3.21). The electricity, which is bought from an energy retailer, is obtained from the National Interconnected System at 34.5 kV

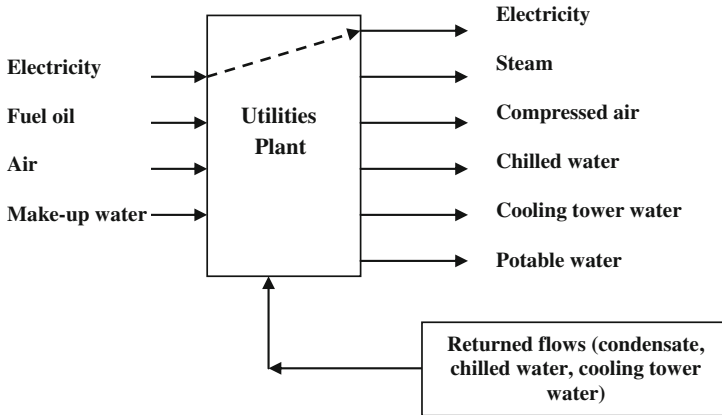
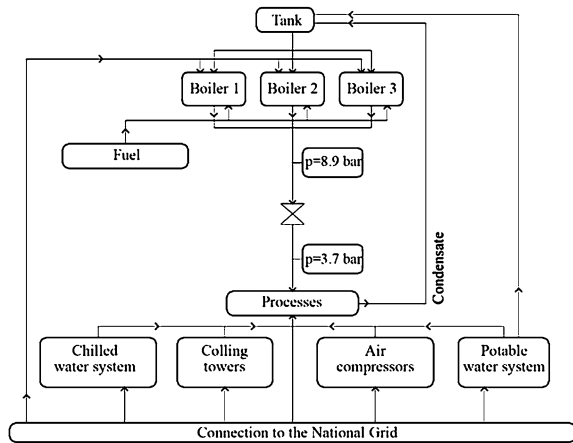


Fig. 3.19 Scheme of the utilities plant [23]

Fig. 3.20 Utilities distribution lines [23]



and transformed to 220 and 440 V. The electricity tariff is negotiated. On October/2000, the plant paid 60.56 US\$/MWh.

- Steam is used to pasteurize, to sterilize, to heat water, and air and for cleaning purposes. It is also used in packing machines and industrial pots, among others. The majority of the applications use the steam enthalpy of condensation at 369.92 kPa and 414.15 K. The average energy demand of steam is 3.42 MW with a peak demand of 5.18 MW (see Fig. 3.21). This represents an average demand of 1.81 kg/s, with a peak demand of 2.42 kg/s. The plant has three boilers (one in stand-by) that can produce 2.49, 2.15, and 1.36 kg/s of steam at 889.80 kPa and 448.15 K, giving a total steam rate of 6 kg/s.
- Chilled water is employed in pasteurizing machines, cooling machines, production tanks, packing machines, cooling rooms, and in the salt water in which

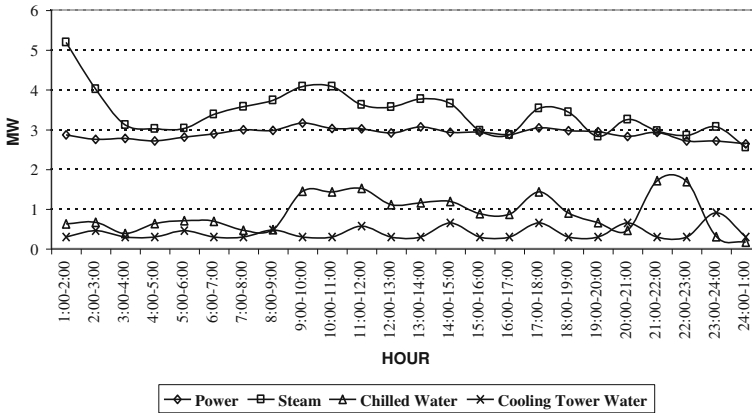


Fig. 3.21 Power, steam, chilled water, and cooling tower water demands [23]

cheese is submersed during manufacture, among others. The average energy demand of chilled water is 893.45 kW with a peak demand of 1705.14 kW (see Fig. 3.21). For the production of chilled water, the plant has an ammonia system composed of three compressors (one of them in stand-by), two evaporative condensers, six expansion valves, and 8 km of pipes. The pipes are submersed in six reservoirs in which water is cooled from 284.18 to 274.15 K, in average. The system has a refrigerating capacity of 1,825 kW.

- Cooling tower water is used in pasteurizing machines and production tanks, among others. It satisfies the cooling needs in processes where the use of chilled water is not required. In other processes, cooling tower water is employed in series with chilled water. The average energy demand of cooling tower water is 389.71 kW with a peak demand of 903.00 kW (see Fig. 3.21). The cooling tower water is produced in a system composed of five cooling towers, which cools water from 308.15 to 296.15 K, in average
- Compressed air is employed in processes, such as pressing, cutting, and packing. The average demand is 0.38 kg/s with a peak demand of 0.45 kg/s (see Fig. 3.22). The plant has a system composed of six compressors that can generate 0.69 kg/s of compressed air at 819.82 kPa, 293.15 K and relative humidity of 85 %.
- Potable water is used in the manufacture of various products, preparation of ferments, and cleaning, among others. The average demand is 15.73 kg/s with a peak demand of 22.10 kg/s (see Fig. 3.22). A system of pumps extracts underground water from four wells. The water is then purified in three parallel treatment plants and stored in tanks. The system can supply 22.69 kg/s of water at 274.94 kPa and 291.15 K.

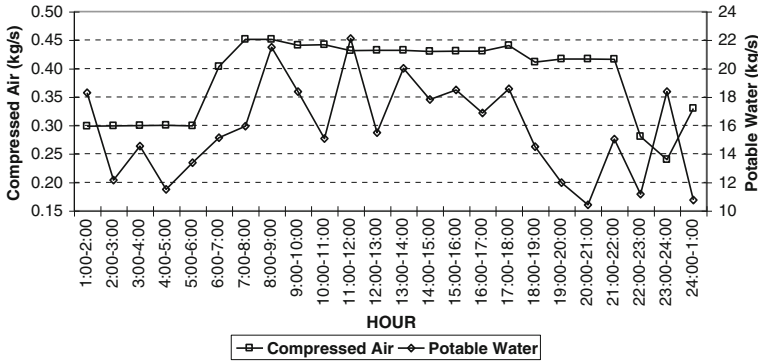


Fig. 3.22 Compressed air and potable water demands [23]

3.5.3 Cogeneration Systems

Figure 3.23 shows a scheme of the cogeneration utilities plant. The cogeneration systems analyzed in this study are: a steam cycle with extraction/condensation steam turbine, a gas turbine based system, and a gas engine-based system.

The steam turbine-based system is composed of an extraction/condensation steam turbine and a high pressure steam generator. The electricity generation capacity is 5 MW. Figure 3.24 shows this configuration. Steam is generated at 4,199 kPa and 596 K. This steam is sent to the extraction/condensation steam turbine and the required steam flow rate, for each hour of the day, is extracted at 400 kPa.

The gas turbine-based system is made up of a gas turbine of the same capacity of the steam turbine (the combustion chamber outlet temperature is 1,295 K) and a waste heat boiler that can produce the required steam flow for each hour at 890 kPa. This configuration is shown in Fig. 3.25.

The gas engine-based system, shown in Fig. 3.26, is made up of a gas engine with an electricity generation capacity of 4.5 MW and a waste heat boiler with a steam generation capacity of 0.75 kg/s at 850 kPa. The remaining steam that is required is generated in the existing boilers.

3.5.4 Comparative Exergy and Thermoeconomic Analysis

The exergy performance of the utilities production systems was quantified by calculating the overall exergy efficiency of the plants [3, 15].

The exergy efficiencies were calculated for the utilities plant in its original operating condition and with the described cogeneration systems. Their values are presented in Table 3.17. The reference atmosphere has a pressure of 74 kPa, temperature of 291 K, and relative humidity of 75 %.

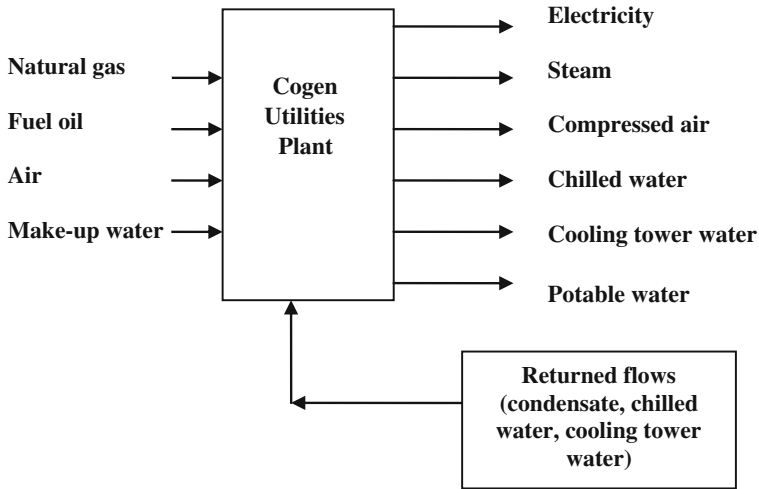
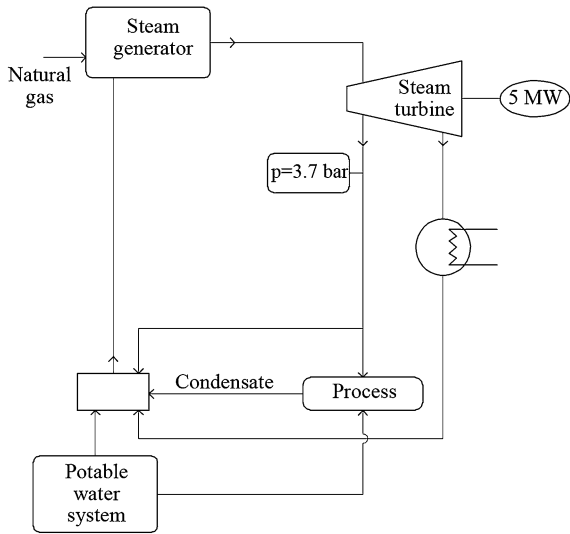


Fig. 3.23 Cogeneration utilities plant [23]

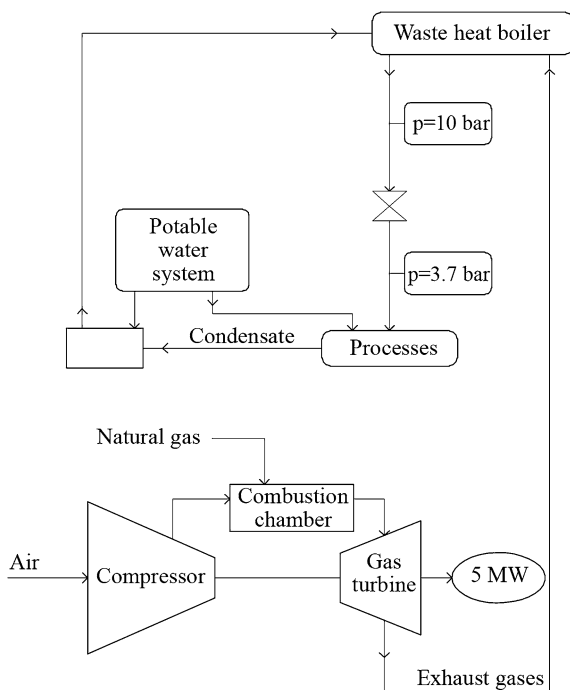
Fig. 3.24 Extraction/condensation steam turbine-based cogeneration system [23]



The gas turbine and the gas engine-based systems present the best exergy efficiency values. The exergy efficiency of the steam turbine-based system is smaller than the original one because in the calculation of the exergy efficiency of the original system it was not considered the fuel required to generate the purchased electricity.

The performance behavior of the plant in the original operating condition and for each one of the considered operating scenarios of the cogeneration plants was simulated by modeling all the processes with the aid of the software EES® [12].

Fig. 3.25 Gas turbine-based cogeneration system [23]



The corresponding production costs of each utility and the costs of the utilities streams along the plant were estimated in an hourly basis.

The production costs of electricity and steam generated in the cogeneration systems were calculated based on programs also implemented in the software EES[®] [12].

The following parameters were used in the thermoeconomic assessment of the cogeneration systems [14]:

- Steam turbine-based system cost (including installation and commissioning costs): US\$5,694,000
- Gas turbine-based system cost (including installation and commissioning costs): US\$3,139,500
- Gas engine-based system cost (including installation and commissioning costs): US\$4,680,000
- Connection to the gas grid: US\$22,682
- Annual operational and maintenance costs: 10 % of investment cost
- Natural gas price: 2.5, 3.5 and 4.5 US\$/MMBtu
- Interest rate: 9 % per year
- Capital recovery period: 10 years
- Load factor: 0.89
- Average operation time: 7,796 h/year
- Inflation is not considered

The original natural gas price was 4.5 US\$/MMBtu.

Fig. 3.27 Mean electricity cost [23]

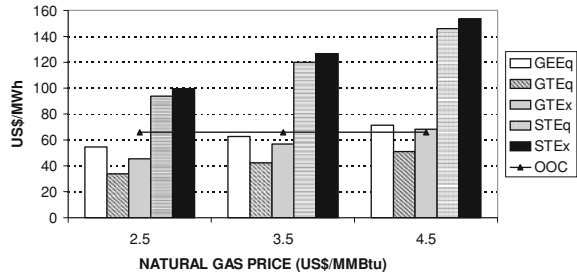
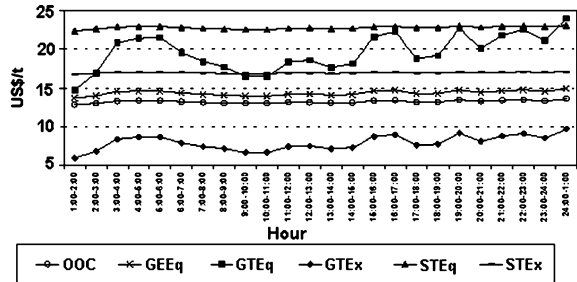


Fig. 3.28 Steam cost for natural gas at 3.5 US\$/MMBtu [23]



The steam production costs are presented for the 24 h of the day because, for the gas turbine-based cogeneration system, the quantity of steam generated and consequently the investment cost per unit of mass varies appreciably. With natural gas at 3.5 US\$/MMBtu, only the gas turbine-based system with the extraction method can produce steam at a lower cost than the original operating condition (OOC), as shown in Fig. 3.28.

The economic performance of the systems can be assessed by means of the total cost rate (TCR) of the systems, considering the investment cost (including the costs of the equipment, installation, and connection to the gas pipeline, operation and maintenance) and the cost associated to the fuel:

$$TCR = I + c_{fuel} B_{fuel} \quad (3.19)$$

Table 3.18 presents the TCR for the analyzed cogeneration systems and for the three natural gas prices.

These values can be compared with 268.39 US\$/h, corresponding to the TCR in the original operating condition. Only the gas turbine-based system with natural gas at 2.5 US\$/MMBtu presents a TCR somewhat lower.

As the considered cogeneration systems produce more electricity than is required in the plant. Then, the surplus could be negotiated in the Colombian Electricity Pool or directly with an electricity retailer or a nonregulated user. Taking the mean price in the Electricity Pool during the year 2000 as a reference, a TCR considering these revenues can be obtained, as indicated in Table 3.19.

Again, only the gas turbine-based system with natural gas at 2.5 US\$/MMBtu presents a lower TCR than the reference case.

Table 3.18 Total cost rate (US\$/h) [23]

Natural gas price (US\$/MMBtu)	Steam turbine	Gas turbine	Gas engine
2.5	411.16	267.05	326.45
3.5	503.41	331.68	368.98
4.5	595.76	396.38	411.54

Table 3.19 Total cost rate selling electricity surplus (US\$/h) [23]

Natural gas price (US\$/MMBtu)	Steam turbine	Gas turbine	Gas engine
2.5	380.31	236.20	304.22
3.5	472.55	300.83	346.74
4.5	564.90	365.52	389.31

3.5.5 Concluding Remarks

From a thermoeconomic standpoint it is interesting to note the differences of the utilities costs resulting of different cost partition methods. The utilization of these methods evidences the importance of costs of products in a cogeneration plant according to its objectives.

The results show that the gas turbine-based system can be an alternative for the implementation of cogeneration in the Colombian dairy industry.

The results also indicate that the panorama for the dissemination of the cogeneration technology in the sector is not satisfactory due to the high price of natural gas and relative low price of electricity. This situation could be improved with a natural gas tariff policy that stimulates cogenerator with lower natural prices.

3.6 Exergoeconomic Evaluation of Trigeneration Systems

3.6.1 Introduction

A trigeneration system can be defined as a particular type of combined heat and power system that supplies, simultaneously, mechanical or electrical demand as well as heating and cooling demands, by consuming a single energy source. It is a very effective option of utilizing fuels exergy. Trigeneration systems can be divided into two parts: the combined heat and power unit (CHP), which generates electricity and supplies a given heating demand, and the second part, a compression or absorption chiller, which produces refrigerating effect using electricity and/or heat from the CHP unit. Combined heating and power technology has been in use in industrial applications since the end of nineteenth century. However, the rapid development of the technologies involved through the last decades, made

easier the application of CHP technology in buildings, hotels, hospitals, schools, community heating, or waste treatment sites. Most recent advances incorporate the use of alternative fuels such as hydrogen or biomass, or the exploitation of excess heat converting it to cooling power, that is used in air conditioning or in various industrial processes [16]. Trigeneration plants have become economically viable due to the commercial spread of absorption chillers [17]. Absorption chillers are generally classified as direct or indirect-fired, and as single, double or triple-effect. In direct-fired units, the heat source can be gas or some other fuel that is burned in the unit. Indirect-fired units use steam or some other heat transfer fluid that brings in heat from a separate source, such as a boiler or heat recovered from an industrial process.

Low pressure, steam-driven absorption chillers are available in capacities ranging from 100 to 1,500 TR (ton of refrigeration). Absorption chillers come in two commercially available designs: single-effect and double-effect. Single-effect machines provide a COP of about 0.7 and require about 8.2 kg of steam at 2.0 bar (abs) per TR of cooling capacity. Double-effect machines are about 40 % more efficient, but require higher grade thermal input, using about 4.5 kg of steam at 6.9–10.3 bar (abs) per TR [18].

In short, absorption cooling may fit when a source of free or low-cost heat is available, or if restrictions related to using conventional refrigeration exist. Essentially, the low-cost heat source displaces higher cost electricity in a conventional chiller.

Trigeneration includes various technologies like: gas turbines, steam turbines, combined cycles, internal combustion engines, fuel cells, and Stirling engines. Some works show diverse applications of the trigeneration systems: in super-markets [19], in the petrochemical industry [20], in the food industry [21], and in hospitals [22].

In the study described in this section, an exergy and exergoeconomic comparison of different trigeneration systems, including a tetra-combined one is carried out in order to calculate the efficiencies and exergy-based cost of electricity, steam, and the exergy transferred to chilled water.

3.6.2 Trigeneration Systems

The analysed trigeneration systems are applied to supply the energy requirements of a dairy industry, taking the same Colombian dairy-industry used in Sect. 3.5 as a case study [23]. The industry energy demands are:

- 2.3 MW of electric power;
- 25 kg/s of chilled water at 5 °C (Evaporator capacity: 525 kW);
- 2 kg/s of saturated steam at 5 bar for process.

Five trigeneration system configurations, shown in Figs. 3.29, 3.30, 3.31, 3.32, and 3.33, are modelled and analysed. These configurations are based on:

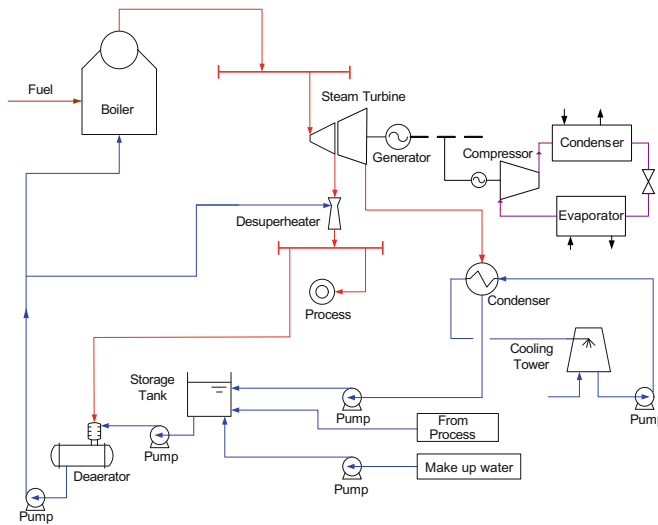


Fig. 3.29 Steam turbine configuration with compression refrigeration system [27]

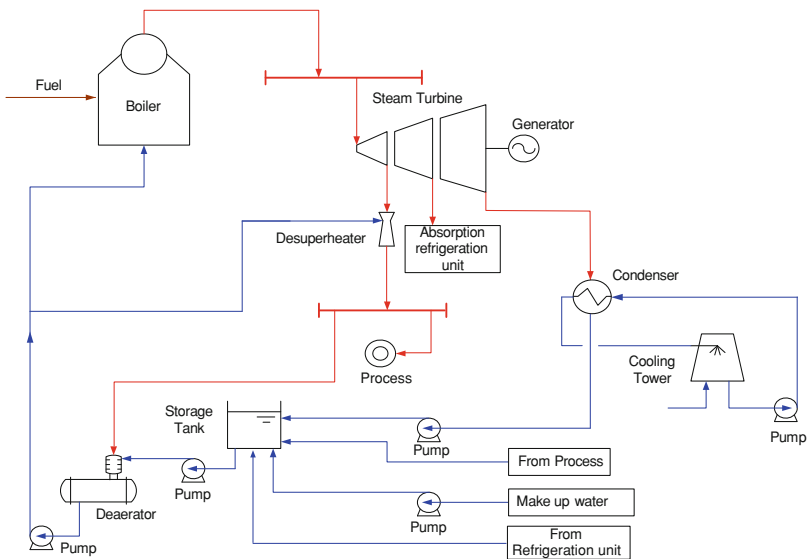


Fig. 3.30 Steam turbine configuration with single effect absorption refrigeration system [27]

- Steam turbine and vapor-compression refrigeration system (Fig. 3.29);
- Steam turbine and single effect absorption refrigeration system (Fig. 3.30);
- Gas turbine and single effect absorption refrigeration system (Fig. 3.31);
- Combined cycle with single effect absorption refrigeration system (Fig. 3.32);
- Tetra combined cycle (Figs. 3.33, 3.34)

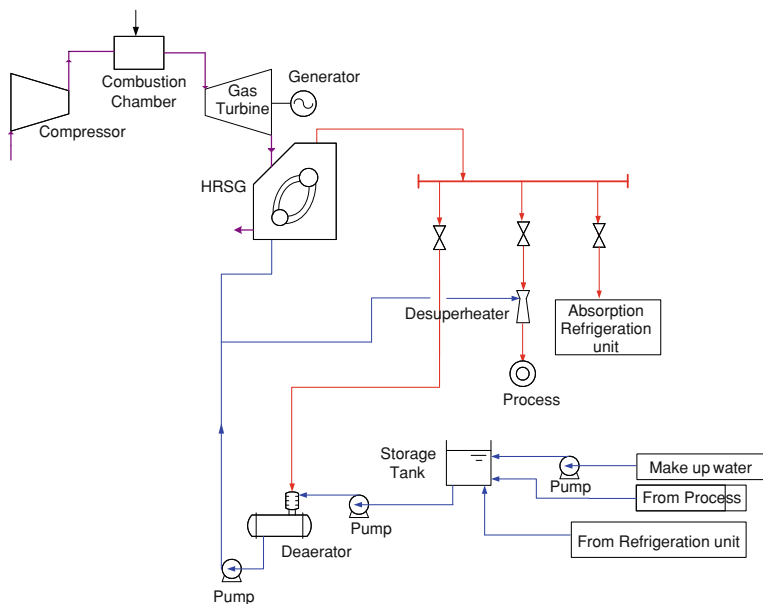


Fig. 3.31 Gas turbine and HRSG with absorption refrigeration system [27]

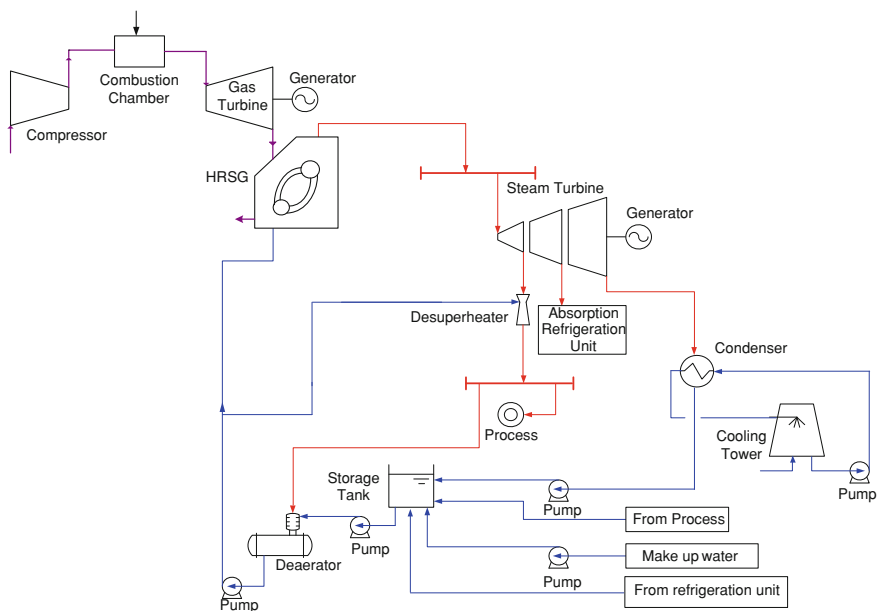


Fig. 3.32 Combined cycle with absorption refrigeration system [27]

Table 3.20 Operational conditions of refrigeration systems [27]

Compression refrigeration system		Absorption refrigeration system	
Compressor power	107.7 kW	Generator solution temperature.	56–81 °C
Condensation temp.	40 °C	Condensation temperature	40 °C
Evaporation temperature	3 °C	Evaporation temperature	3 °C
Refrigerant	R 134a	Absorber solution temperature	60–31 °C
Environmental condition	25 °C and 1 bar	Solution concentrations	58.2–54.2 %
Chilled water inlet temp.	10 °C	Environmental condition	25 °C and 1 bar
Chilled water outlet temp.	5 °C	Chilled water inlet temp.	10 °C
		Chilled water outlet temp.	5 °C

The data set defining operational conditions of compression and absorption refrigeration systems is shown in Table 3.20.

For trigeneration systems operating with steam turbines, the parameters presented in Table 3.21 are taken.

The parameters used to simulate the trigeneration system based on gas turbine and HRSG with single effect absorption refrigeration system are shown in Table 3.22.

Additionally to parameters presented in Table 3.22, data described in Table 3.23 are considered for the simulation of the combined cycle-based trigeneration system.

Figure 3.33 presents the concept of the fifth analysed trigeneration system developed by Garagatti Arriola and Oliveira [24]. This system is composed of a heat engine (working between the temperatures T_{cc} and T_{sc}) coupled in thermal series to a cogeneration system (that receives $(1 - f)Q_2$ and rejects Q_4 , Q_5 and Q_3) and to a hybrid refrigeration system (that receives Q_5 and fQ_2 , rejects Q_6 and Q_8 , providing a cooling effect Q_7). This trigeneration system generates electricity ($W_{gt} + W_{st}$), produces steam/hot water (Q_4) and chilled water (Q_7) to a given industrial process. In some cases, the heat loss to the environment (Q_3) is zero.

The overall energy efficiency, η_e , and the exergy efficiency, η_b , of this trigeneration system can be written as a function of the energy performance parameters of each system of the tetra-combined trigeneration system:

$$\eta_e = \eta_1 + (1 - \eta_2)(\eta_2 - f + f \text{COP}) + r(\text{COP} - 1) \quad (3.20)$$

where:

$$\eta_e = \frac{W_{gt} + W_{st} + Q_4 + Q_7}{Q_1} \quad (3.21)$$

f = the fraction of the rejected heat of the heat engine that is sent to the refrigeration system;

$$\eta_2 = \frac{W_{st} + Q_4 + Q_5}{Q_2(1 - f)} \quad (3.22)$$

$$\text{COP} = \frac{Q_7}{(f Q_2 + Q_5)} \quad (3.23)$$

Table 3.21 Parameters of trigeneration systems operating under Rankine cycle [27]

Parameter	Value
Boiler efficiency (% , LHV basis)	85
Electric generator efficiency (%)	95
Steam pressure (bar)	42
Steam temperature (°C)	420
Turbine stages isentropic efficiency (%)	78–80
Pump isentropic efficiency (%)	70

Table 3.22 Assumed parameters used to simulate the third trigeneration system [27]

Parameter	Value
Turbine inlet temperature (TIT) (°C)	1,200
Compressor isentropic efficiency (%)	85
Gas turbine isentropic efficiency (%)	87
Saturated steam pressure (bar)	10
HRSg heat losses (%)	2
HRSg Pinch (°C)	10
HRSg Approach (°C)	5
Pump isentropic efficiency (%)	70

Table 3.23 Additional parameters to simulate the combined cycle and absorption refrigeration system based trigeneration system [27]

Parameter	Value
Electric generator efficiency (%)	95
Steam pressure (bar)	42
Steam temperature (°C)	420
Turbine (condensing–extraction) isentropic efficiency (%)	78–80
Pump isentropic efficiency (%)	70

$$r = \frac{Q_5}{Q_1} \quad (3.24)$$

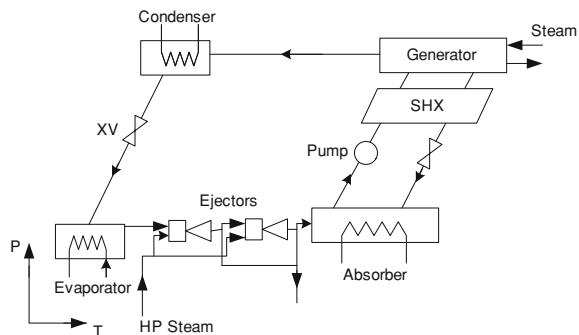
Equation 3.20 shows the influence of the performance parameter of each component, as well as the rejected heat distribution, in the overall performance of the cogeneration system.

The exergy efficiency, η_b , of this trigeneration system is done by Eq. 3.25:

$$\eta_b = \frac{W_{gt} + W_{st} + Q_4 \theta_4 + Q_7 \theta_7}{Q_1 \theta_1} \quad (3.25)$$

The tetra-combined trigeneration system is composed of three subsystems in thermal cascade: gas turbine, a cogeneration system based on a steam cycle and a hybrid absorption ejecto-compression chiller. The expression tetra-combined is derived from the fact of this system to be based on two power cycles (Brayton and Rankine) and two refrigeration technologies (absorption and ejecto-compression).

Fig. 3.35 Absorption-ejecto compression refrigeration system Dühring chart schematic [28]



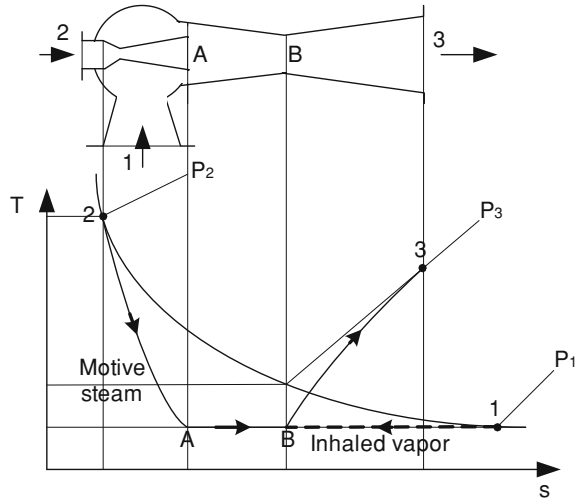
In tetra-combined trigeneration system, the gas turbine produces power and it uses natural gas as energy source. The cogeneration subsystem, based on a steam cycle, uses the rejected gases from the gas turbine to produce superheated steam in a HRSG. The superheated steam feeds an extraction/condensation steam turbine. The steam turbine produces power and has three steam extractions. The first extraction is to feed the ejectors of the hybrid absorption ejecto-compression chiller; the second one is imposed by the process. This process steam is highly superheated and in certain applications saturated steam is needed, so it is necessary to include a desuperheater to take the superheated steam down to the saturated state. In the desuperheater a mixture of superheated steam and water is produced and therefore the saturated steam is obtained. The third steam extraction in turbine is used as heat source to feed the generator of hybrid absorption ejecto-compression chiller. The remaining steam goes out from turbine and enters in the condenser to be recovered like feed water for boiler.

Figure 3.34 shows a schematic diagram of the tetra-combined trigeneration system.

The absorption ejecto-compression refrigeration system had its origin in the work of Oliveira and Le Goff [25]. The system is characterized by having ejectors between the evaporator and absorber. The operation is similar to the single-effect absorption system, with the variation of using ejectors. The number of ejectors depends on the steam pressure decrease required in the evaporator and the steam pressure increase required in the absorber. Each ejector operates with a pressure ratio of about two. The ejector exhaust is discharged to the absorber, causing the absorber pressure to be at a higher level than that in the evaporator. Therefore, the solution within the absorber can be kept away from crystallization when the system is needed to operate with low evaporator temperature or with high absorber temperature such as an air-cooled unit. Figure 3.35 shows a water/lithium-bromide absorption ejecto-compression refrigeration system.

The processes inside the ejector are represented in Fig. 3.36. The refrigerant vapor at low pressure enters the ejector at point 1, and it is drawn by means of the expansion of the high pressure steam at point 2 that produces a vacuum when it flows in the ejector from point 2 and proceeds up to point A, increasing the refrigerant vapor pressure to point 3. This steam at the exit of the first ejector is

Fig. 3.36 Evolution of motive steam and drawn vapour throughout ejector [29]



used by a second ejector to lift up the refrigerant vapor pressure up to the absorber pressure. Steam then is absorbed by the strong solution coming from the generator, and this diluted solution is sent back to generator by means of the solution pump.

To reduce the motive steam consumption, in each ejector exit there is a mass flow rate deviation that is sent again to the boiler, or used in another process, if the pressure conditions allows.

3.6.3 Modelling and Simulation of Trigeneration Systems

The models presented before were implemented in the software EES[®] [12], and simulated considering steady-state operation.

For the purpose of analysis of absorption refrigeration systems, the following assumptions are made:

- The analysis is made under steady state conditions;
- The refrigerant at the outlet of the condenser is saturated liquid;
- The refrigerant at the outlet of the evaporator is saturated vapor;
- The outlet temperatures from the absorber and from generators correspond to equilibrium conditions of the mixing and separation, respectively;
- Pressure losses in the pipelines and in heat exchangers are negligible;
- Heat exchanges between the system and surroundings, other than the prescribed at the generator, high temperature generator (in double-effect absorption system), evaporator, condenser, and absorber, are negligible;
- The reference environmental is at 25 °C (T_0) and 1 bar (P_0).

In hybrid absorption ejecto-compression chiller, the following assumptions were considered for ejectors energy balance:

- Adiabatic flow;
- The kinetic energy in Chaps. 1, 2 and 3 of the ejector is negligible;
- 1D flow;
- Steady state condition;
- The saturation pressure at the mixing region of vapors (point A to point B of Fig. 3.36) is constant.

The hybrid absorption ejecto-compression refrigeration system was modeled with two ejectors connected in series flow arrangement and using a pressure ratio of 1.8 for each one.

The production costs were evaluated considering the exergy-based cost for fuel equal to 1 kJ/kJ. For distribution costs in control volumes with more than one product, the equality criterion was adopted (see Chap. 2). That is, each product has the same importance and consequently their exergy-based cost were set equal (i.e. electricity and process steam, in cogeneration systems). Thus, the cost associated to the irreversibility in the control volume is distributed equally among the exergy content of the outlet product flows.

3.6.4 Results

The performance results are presented and discussed for three energy requirements scenarios [26]:

- in the first scenario steam turbine configurations supply the plant requirements (2.3 MW of electric power, 25 kg/s of chilled water at 5 °C, and 2 kg/s of saturated steam at 5 bar for process);
- the second one includes a gas turbine with HRSG and absorption refrigeration system capable to generate 1,800 kW of electricity surplus;
- the third one includes a combined cycle with absorption refrigeration system and the tetra-combined trigeneration system generating 7,500 kW of electricity surplus.

For the described configurations, the energy and exergy efficiencies are calculated according to Eqs. 3.26 and 3.27, and the results are presented in Tables 3.24, 3.25 and 3.26.

$$\eta_e = \frac{W_{\text{plant}} + W_{\text{excess}} + Q_{\text{process}} + Q_{\text{chilledwater}}}{m_{\text{fuel}} \text{LHV}} \quad (3.26)$$

$$\eta_b = \frac{W_{\text{plant}} + W_{\text{excess}} + \Delta B_{\text{process}} + \Delta B_{\text{chilledwater}}}{m_{\text{fuel}} b_{\text{fuel}}} \quad (3.27)$$

where W_{plant} is the electric dairy demand, W_{excess} is the excess generated electricity that can be sold to the grid, Q_{process} is the heating process demand, $Q_{\text{chilledwater}}$ is the cooling demand, m_{fuel} is the fuel mass flow rate and LHV is the lower heating

Table 3.24 Energy and exergy efficiency of trigeneration systems based on steam turbine [28]

Trigeneration system	η_e (%)	η_b (%)
Steam turbine with compression refrigeration system	56.88	26.64
Steam turbine with absorption refrigeration system	57.37	26.87

Table 3.25 Energy and exergy efficiency of trigeneration systems with 1,800 kW excess electricity [28]

Trigeneration system	η_e (%)	η_b (%)
Steam turbine with compression refrigeration system	44.89	25.23
Steam turbine with absorption refrigeration system	45.28	25.45
Gas turbine and HRSG with absorption refrigeration system	79.12	44.65

Table 3.26 Energy and exergy efficiency of trigeneration systems with 7,500 kW excess electricity [28]

Trigeneration system	η_e (%)	η_b (%)
Steam turbine with compression refrigeration system	33.53	23.90
Steam turbine with absorption refrigeration system	33.82	24.11
Combined cycle with absorption refrigeration system	65.45	46.21
Tetra-combined cycle	65.79	46.45

value, $\Delta B_{\text{process}}$ is the exergy flow rate variation of process steam, $\Delta B_{\text{chilledwater}}$ is the exergy flow rate variation of chilled water, and b_{fuel} is the fuel specific exergy.

In order to show the results of exergoeconomic study for the trigeneration systems, the fuel exergy rate, exergy destruction rate, and exergy-based costs for each configuration were calculated and discussed next.

Figure 3.37 shows fuel exergy rate (kW) of each studied configuration for the analyzed scenarios: without and with electricity surplus.

As Fig. 3.37 shows, fuel exergy rate for configuration using steam turbines systems is very similar, in all cases, with a small advantage for the cycle with absorption refrigeration system. In the second scenario, gas turbine with HRSG and absorption refrigeration system presents a reduction in fuel exergy rate, around 44 %, with respect to steam turbine configurations.

For 7,500 kW excess electricity generation, combined cycle with absorption refrigeration system and tetra-combined cycle present important reduction (around 48 %) of fuel exergy rate with respect to steam turbine with compression and absorption refrigeration systems, respectively.

Figure 3.38 shows the exergy destruction rate caused by systems operation for all studied cases.

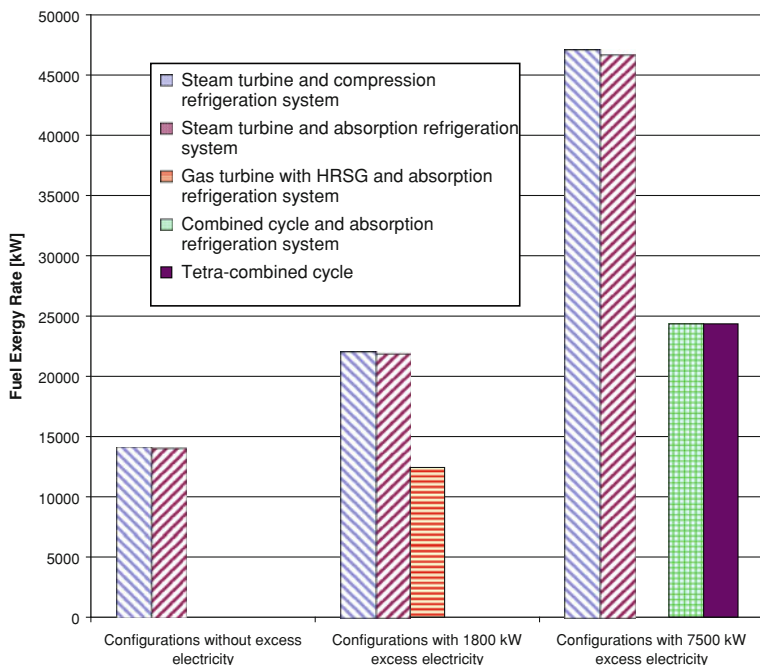


Fig. 3.37 Fuel exergy rate comparison for the analyzed systems [28]

A comparative analysis of the studied systems, shown in Fig. 3.38 is similar to the one presented in Fig. 3.37. The exergy destroyed rate by the system with steam turbine with compression refrigeration system is slightly higher than the configuration with steam turbine and absorption refrigeration system, for all analyzed cases. For 1,800 kW of electricity surplus, gas turbine with HRSG and absorption refrigeration system presents a reduction in exergy destruction of around 63 % with respect to steam turbine configurations. For 7,500 kW of electricity surplus, the exergy destroyed by tetra-combined cycle is lightly lower than combined cycle with absorption refrigeration system and also a reduction of exergy destruction around of 71 % with respect to steam turbine with compression and absorption refrigeration systems.

Exergy-based costs (kJ/kJ) of electricity, process steam and exergy transferred to chilled water for the studied configurations in the three operating scenarios are summarized in Fig. 3.39.

In Fig. 3.39 it can be concluded that without electricity surplus, the exergy-based cost of electricity and process steam are similar in steam turbine configurations, being slightly higher in the system with compression refrigeration system. The comparison for chilled water cost between these two configurations is interesting, since in the first case, exergy based cost is 11.3 kJ/kJ, whereas with absorption cycle it is 19.55 kJ/kJ. The reason for this difference is due to the values

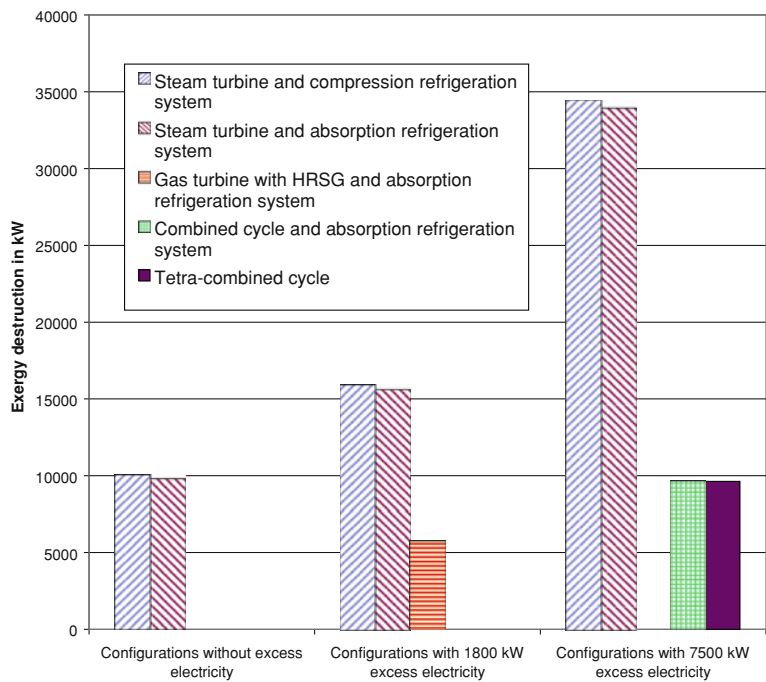


Fig. 3.38 Exergy destruction for the different systems [28]

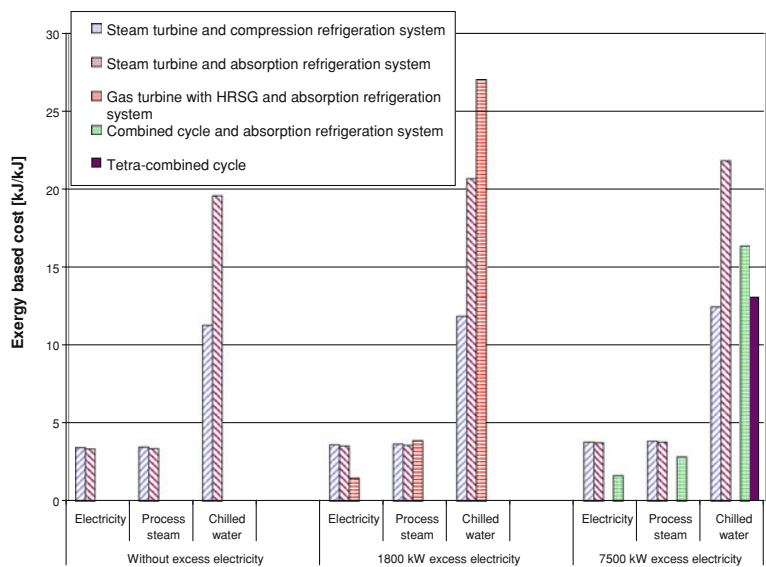


Fig. 3.39 Exergy-based costs (kJ/kJ) of electricity, process steam and chilled water for the studied configurations [28]

Table 3.27 Average exergy-based cost of products for trigeneration system based on steam turbine [28]

Trigeneration system	Average exergy cost (kJ/kJ)
Steam turbine with compression refrigeration system	3.75
Steam turbine with absorption refrigeration system	3.72

Table 3.28 Average exergy-based cost of products for trigeneration system with 1,800 kW excess electricity [28]

Trigeneration system	Average exergy cost (kJ/kJ)
Steam turbine with compression refrigeration system	3.96
Steam turbine with absorption refrigeration system	3.93
Gas turbine and HRSG with absorption refrigeration system	2.24

Table 3.29 Average exergy-based cost of products for trigeneration system with 7,500 kW excess electricity [28]

Trigeneration system	Average exergy cost (kJ/kJ)
Steam turbine with compression refrigeration system	4.18
Steam turbine with absorption refrigeration system	4.14
Combined cycle with absorption refrigeration system	2.17
Tetra-combined cycle	2.15

of the exergy efficiency of these cycles: 30.41 % for compression refrigeration system, and 17.14 % for the absorption refrigeration system.

In the 1,800 kW electricity surplus scenario, the gas turbine with HRSG and absorption refrigeration system has lower electricity exergy-based cost than steam turbine configurations. For process steam the exergy-based cost is very similar for the three analyzed configuration. Regarding the exergy transferred to chilled water, the highest cost is given by the gas turbine configuration. This happens because the steam exergy-based cost entering the generator of absorption refrigeration system has an exergy-based cost of 5.4 kJ/kJ and also because of the low chiller exergy efficiency (17.14 %). However, the gas turbine with HRSG and absorption refrigeration system presents higher global plant exergy efficiency as can be seen in Table 3.25.

In the last scenario, the electricity exergy-based costs, shown in Fig. 3.39 are the average values, calculated taking into account the power developed by the steam and gas turbines. The combined cycle and Tetra-combined cycle present considerable reduction in electricity and process steam exergy-based costs in comparison with steam turbine configuration. In this scenario, the biggest

reduction in the exergy-based cost of chilled water is presented in the Tetra-combined cycle, as consequence of having an exergy efficiency in the hybrid absorption ejecto-compression chiller of 21.24 %, in contrast with the exergy efficiency of the single effect absorption chiller of combined cycle, 17.14 %, showing an advantage of including ejectors between the evaporator and absorber.

Tables 3.27, 3.28 and 3.29 show the average exergy-based cost of products for the different studied configurations.

In general, observing the impact in the formation of energy conversion costs for the proposed configurations, the minor impact in exergy-based costs of products (electricity, process steam and exergy transferred to chilled water) is for the Tetra-combined cycle, as it is possible to appreciate looking at the average exergy-based costs of the different configurations on Tables 3.27, 3.28 and 3.29.

Nevertheless, to choose an alternative or another, it is also necessary to take into consideration technical and financial aspects, since better exergy-based costs are directly linked to the efficiency of the energy conversion processes.

3.6.5 Concluding Remarks

Trigeration represents a quite interesting alternative of producing electricity and reducing the production costs of utilities. In this comparative study, an analysis of different trigeration systems was done, including a tetra-combined system, by means of the use of exergoeconomic analysis to quantify its energy and exergy efficiency and the impact in the production of electricity, process steam and chilled water for air conditioning purposes. The preliminary performance results of the studied trigeration systems show the viability of tetra-combined cycle. This system has higher exergy efficiency than the single effect absorption chiller. This configuration also presents a bigger impact in the exergy-based cost of chilled water in comparison with other analyzed systems.

References

1. Szargut J, David RM, Steward F (1988) Exergy analysis of thermal, chemical, and metallurgical processes. Hemisphere Publishing, New York
2. Bejan A (1988) Advanced engineering thermodynamics. Wiley, New York
3. Oliveira S Jr, Van Hombeeck H (1997) Exergy analysis of petroleum separation processes in offshore platforms. *Energy Convers Manage* 38:1577–1584
4. Beyer J (1970) Strukturuntersuchungen-notwendiger Bestandteil der effektivitätsanalyse von wärmeverbrauchersysteme. *Energieanwendung* 19:358–361
5. Borelli SJS, Oliveira S Jr (2008) Exergy based method for analysing the composition of the electricity cost generated in gas-fired combined cycle plants. *Energy* 33:153–162
6. Means RS (2002) Mechanical cost data. RS Means Company, Inc., EUA—2002
7. Boehm RF (1987) Design analysis of thermal systems. Wiley, New York
8. GATECYCLE software, v.5.5.1 (2003) General Electric Power Systems Inc.

9. Means RS (1998) Ministry of mines and energy. In: National energy balance, Brasília (In Portuguese)
10. Tolmasquim M et al (1999) Evaluation of technical and economic potentials and difficulties identification to the use of cogeneration in selected sectors in Brazil. In: PROCEL/COOPE, Rio de Janeiro (In Portuguese)
11. Teixeira MS, Oliveira S Jr (2001) Thermoeconomic evaluation of cogeneration systems for a chemical plant. *Int J Thermodyn* 4:157–163
12. Klein SA (2011) Engineering equation solver—EES, F-Chart Software, www.fChart.com
13. Cespedes JFP, Oliveira S Jr (1995) Cogeneration in the Brazilian tertiary sector: exergetic and thermoeconomic analysis. In: Proceedings of the 8th international conference on efficiency, costs, optimization, simulation and environmental impact of energy systems, Istanbul
14. Larrazábal ML (2001) Thermoeconomic analysis of the use of cogeneration with natural gas in the Colombian dairy industry. Masters on Energy Dissertation, University of São Paulo, São Paulo, Brazil (In Portuguese)
15. Tsatsaronis G (1995) On the efficiency of energy systems In: Proceedings of the 8th international conference on efficiency, costs, optimization, simulation and environmental impact of energy systems, Istanbul
16. Kavvadias KC, Tosios AP, Maroulis ZB (2010) Design of a combined heating, cooling and power system: sizing, operation strategy selection and parametric analysis. *Energy Convers Manag* 51:833–845
17. Cardona E, Piacentino A (2003) A methodology for sizing a trigeneration plant in Mediterranean areas. *Appl Therm Eng* 23:1665–1680
18. Absorption Chillers (2010) Available at: <http://www.absorptionchillers.com/>. Cited Jan 2010
19. Maidment GG, Tozer RM, Missenden JF (2001) Combined cooling, heat and power (CCHP) in Supermarkets. In: Heat powered cycles conference, conservatoire national des arts et métiers, Paris
20. Colonna P, Gabrielli S (2003) Industrial trigeneration using ammonia-water absorption refrigeration systems (AAR). *Appl Therm Eng* 23:381–396
21. Bassols J, Kuckelkorn B, Langreck J et al (2002) Trigeneration in the food industry. *Appl Therm Eng* 22:595–602
22. Ziher D, Poredos A (2006) Economics of trigeneration system in a hospital. *Appl Therm Eng* 26:680–687
23. Larrazábal ML, Oliveira S Jr (2002) Thermoeconomic evaluation of cogeneration systems for a dairy industry. In: Proceedings of the 18th international conference on efficiency, costs, optimization, simulation and environmental impact of energy systems, Berlin
24. Garagatti Arriola DW, Oliveira S Jr (2001) Tetra-combined cogeneration system. Exergy and thermoeconomic analysis. In: Proceedings of the congress HPC'01—cooling, heating and power systems, Paris
25. Oliveira S Jr, Le Goff P (1993) Hybrid systems absorption-compression to upgrade industrial waste heat. In: In: Proceedings of the energy systems and ecology proceedings of the international conference, Krakow
26. Burbano JC, Pellegrini LF, Oliveira S Jr (2009) Comparative exergoeconomic analysis of trigeneration systems for a dairy industry. In: Proceedings of the 22nd international conference on efficiency, costs, optimization, simulation and environmental impact of energy systems, Foz de Iguaçu
27. Burbano JC (2011) Exergoeconomic optimization of tetra-combined trigeneration system. Ph.D. Thesis Polytechnic School of the University of São Paulo, São Paulo, Brazil (In Portuguese)
28. Burbano JC, Pellegrini LF, Oliveira S Jr (2010) Exergoeconomic analysis of tetra-VCombined trigeneration systems. In: Proceedings of the 23rd international conference on efficiency, costs, optimization, simulation and environmental impact of energy systems, Lausanne

29. Oliveira S Jr (1991) Upgrading industrial thermal effluents—Exergetic, entropic and economic analysis. Ph.D. Thesis. Polytechnic National Institute of Lorraine, Nancy (In French)
30. Borelli SJS (2005) Method for the analysis of the composition of electricity costs in combined cycle thermoelectric power plants. Master Dissertation, Institute of Eletrotechnical and Energy, University of Sao Paulo, São Paulo, Brazil (In Portuguese)
31. Gas Turbine World Handbook 2004–2005, Volume 24—Pequot Publications, 2005